

Non-hydrostatic modeling with IFS: current status

**Nils Wedi, Pierre Benard, Karim Yessad, Agathe Untch,
Sylvie Malardel, Mats Hamrud, George Mozdzynski, Mike Fisher,
and Piotr Smolarkiewicz**

Many thanks to all ECMWF colleagues ...

Outline

- ◆ **Overview of the current status of non-hydrostatic modelling at ECMWF**
- ◆ **Identify main areas of concern and their suggested resolve**
 - ◆ **The spectral transform method**
 - ◆ **Compressible vs. unified hydrostatic-anelastic equations**
- ◆ **Conclusions**

Introduction – A history

- ◆ Resolution increases of the deterministic 10-day medium-range Integrated Forecast System (IFS) over ~25 years at ECMWF:
 - ◆ 1987: T 106 (~125km)
 - ◆ 1991: T 213 (~63km)
 - ◆ 1998: T_L319 (~63km)
 - ◆ 2000: T_L511 (~39km)
 - ◆ 2006: T_L799 (~25km)
 - ◆ 2010: T_L1279 (~16km)
 - ◆ 2015?: T_L2047 (~10km)
 - ◆ 2020-???: (~1-10km) Non-hydrostatic, cloud-permitting, substantially different cloud-microphysics and turbulence parametrization, substantially different dynamics-physics interaction ?

The Athena Project (6 months)

An example of the computational efficiency of the hydrostatic IFS

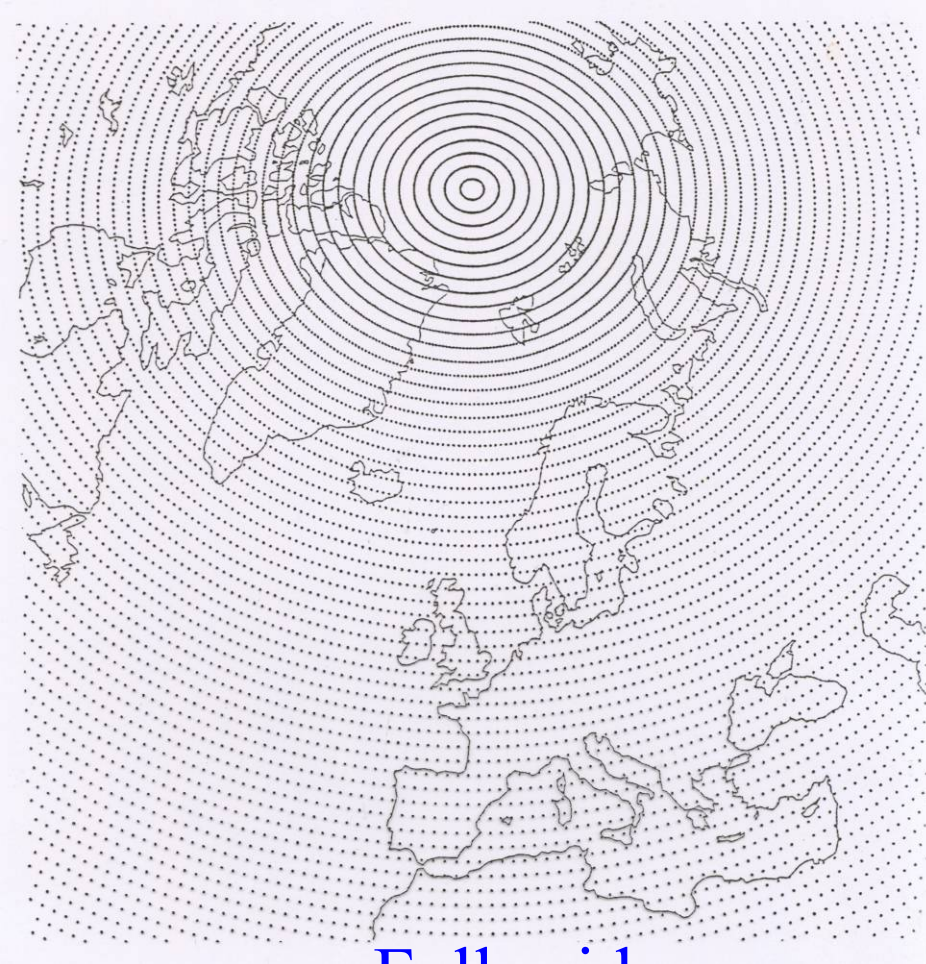
- ◆ IFS (cycle 36r1) atmosphere-only runs with prescribed SST data from observations until 2007 (2070- A1B scenario SST forcing comes from CCSM simulation)
- ◆ Set of 13-months long integrations (1960-2007) and AMIP long runs (1960-2007 and 2070-2117)
 - ◆ $T_{L159L91}$ (~125 km, $\Delta t = 3600s$) **3 x 47 years**
 - ◆ $T_{L511L91}$ (~39 km, $\Delta t = 900s$) **1 x 47 years**
 - ◆ $T_{L1279L91}$ (~16 km, $\Delta t = 600s$) **3 x 47 years**
 - ◆ $T_{L2047L91}$ (~10 km, $\Delta t = 450s$) **1x 19 years**
- ◆ Factor 10-15 larger time-step compared to existing state-of-the-art non-hydrostatic models at equivalent resolutions, additional savings from the reduced grid (~30%) and the direct solver in the semi-implicit scheme.

Ultra-high resolution global IFS simulations

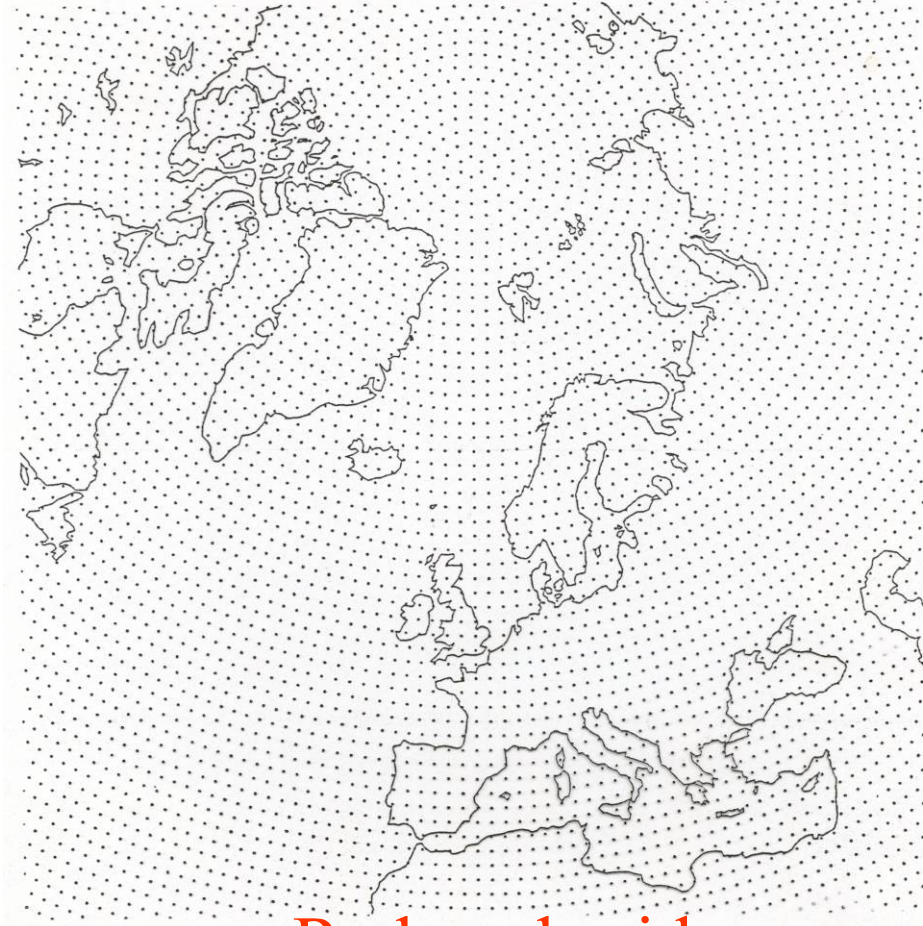
- ◆ T_L0799 (~ 25km) >> 843,490 points per field/level
- ◆ T_L1279 (~ 16km) >> 2,140,702 points per field/level
- ◆ T_L2047 (~ 10km) >> 5,447,118 points per field/level
- ◆ T_L3999 (~ 5km) >> 20,696,844 points per field/level (**world record** for spectral model ?!)

The Gaussian grid

About 30% reduction in number of points



Full grid



Reduced grid

Reduction in the number of Fourier points at high latitudes is possible because the associated Legendre functions are very small near the poles for large m .

Preparing for the future: The **nonhydrostatic IFS**

- ◆ Developed by Météo-France and its ALADIN partners *Bubnová et al., (1995); ALADIN (1997); Bénard et al. (2004,2005,2010)*
- ◆ Made available in IFS/Arpège by Météo-France (*Yessad, 2008*)
- ◆ Testing of NH-IFS described in Techmemo TM594 (*Wedi et al. 2009*)

Two new prognostic variables in the nonhydrostatic formulation

$$Q \equiv \log(p/\pi)$$

‘Nonhydrostatic
pressure departure’

$$d \equiv -g(p/mRT)\partial w/\partial\eta \quad \text{‘vertical divergence’}$$

Define also: $\mathcal{D} \equiv d + \mathcal{X}$

With residual residual

$$\mathcal{X} \equiv (p/RTm)\nabla_{\eta}\Phi \cdot \partial\mathbf{v}_h/\partial\eta$$

Three-dimensional divergence writes

$$D_3 = \nabla_{\eta} \cdot \mathbf{v}_h + \mathcal{X} + d.$$

NH-IFS prognostic equations

$$\frac{d\mathbf{v}_h}{dt} = -\frac{RT}{p}\nabla_\eta p - \frac{1}{m}\frac{\partial p}{\partial\eta}\nabla_\eta\Phi - 2\Omega \times \mathbf{v}_h + P_v,$$

$$\frac{dD}{dt} = \frac{dd}{dt} + \frac{d\mathcal{X}}{dt} = -\frac{gp}{mRT}\frac{\partial P_w}{\partial\eta},$$

$$\frac{dT}{dt} = -\frac{RT}{c_v}D_3 + \frac{c_p}{c_v}P_T,$$

$$\frac{dQ}{dt} = -\frac{c_p}{c_v}D_3 - \frac{1}{\pi}\frac{d\pi}{dt} + \frac{c_p}{c_v\Gamma}P_T.$$

$$\frac{\partial\pi_s}{\partial t} = -\int_0^1 \nabla_\eta \cdot (m\mathbf{v}_h)d\eta,$$

‘Physics’

— “anelastic physics coupling”

The planet ...

$$a < a_{Earth}$$

(Smolarkiewicz et. al. 1998;
Wedi and Smolarkiewicz, 2009)



Scale analysis for NH local-scale problems

$\delta = 0, \Gamma = 1$
shallow atmosphere approximation

$$\frac{du}{dt} = 2\Omega(v \sin \phi - \delta w \cos \phi) + \frac{uv}{\Gamma a} \tan \phi - \delta \frac{uw}{\Gamma a} - \frac{1}{\rho \Gamma a \cos \phi} \frac{\partial p}{\partial \lambda}$$

$$\frac{dv}{dt} = -2\Omega u \sin \phi - \frac{u^2}{\Gamma a} \tan \phi - \delta \frac{vw}{\Gamma a} - \frac{1}{\rho \Gamma a} \frac{\partial p}{\partial \phi}$$

U^2/L	$f_0 U$	$f_0 W$	U^2/a	UW/a	$\Delta p / \rho L$
10^{-1}	10^{-3}	10^{-4}	10^{-3}	10^{-4}	10^{-1}

$a \sim 100 \text{ km}$

$$\frac{dw}{dt} = \delta 2\Omega u \cos \phi + \delta \frac{u^2 + v^2}{\Gamma a} - \frac{1}{\rho} \frac{\partial p'}{\partial r} - g \frac{\rho'}{\rho}$$

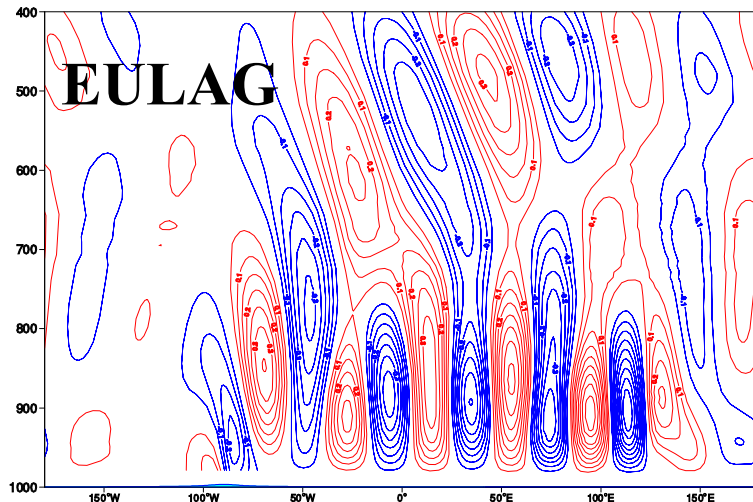
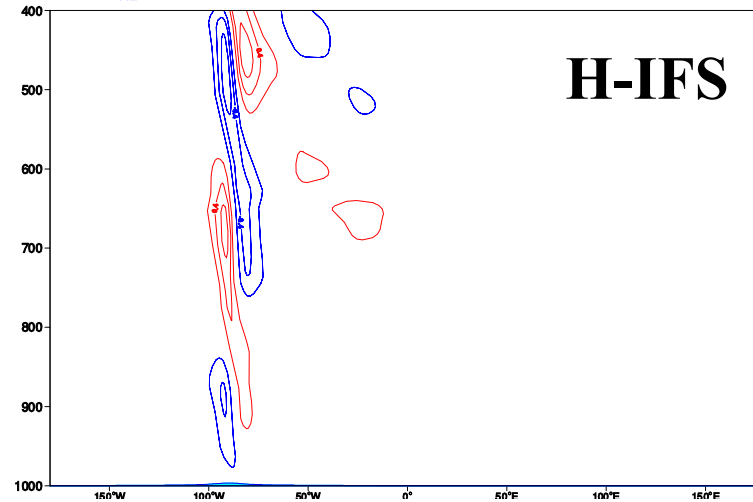
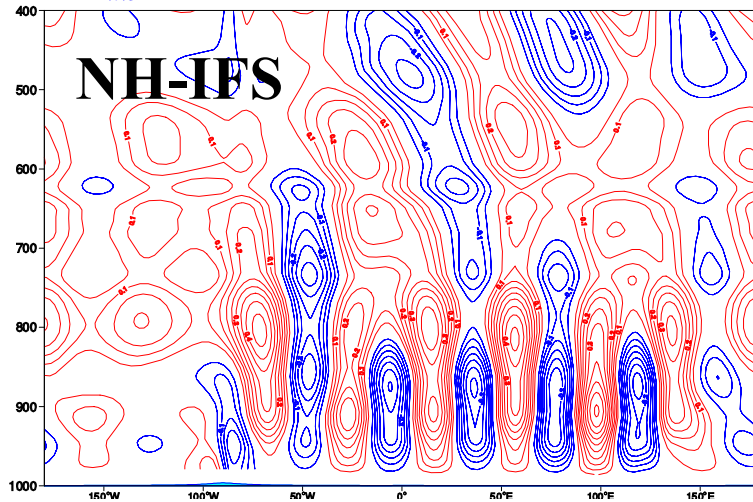
UW/L	$f_0 U$	U^2/a	$dP' / \rho H$	$N^2 H$
10^{-2}	10^{-3}	10^{-3}	10^{-2}	10^{-2}

$a \sim 100 \text{ km}$

Test-bed for NH effects

- ◆ **3D global simulations, without the prohibitive cost, when resolving non-hydrostatic effects.**
- ◆ **Study the influence of the model formulation and/or various numerical choices on selected wave-types in three dimensions.**
- ◆ **Use of the established vertical discretization and/or physical parameterization packages.**
- ◆ **Use of the existing optimized 3D code framework.**

Quasi two-dimensional orographic flow with linear vertical shear

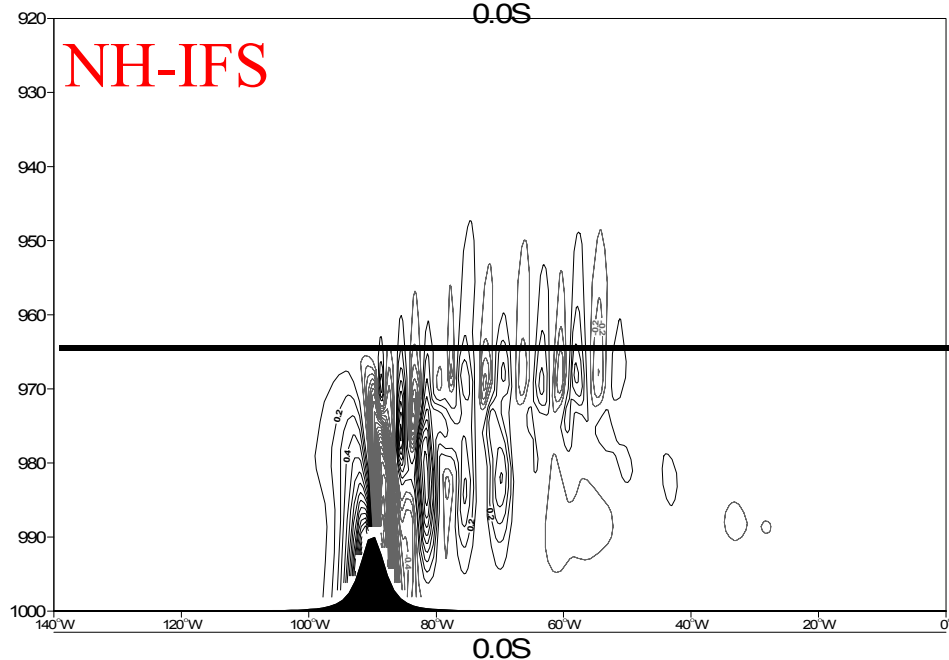
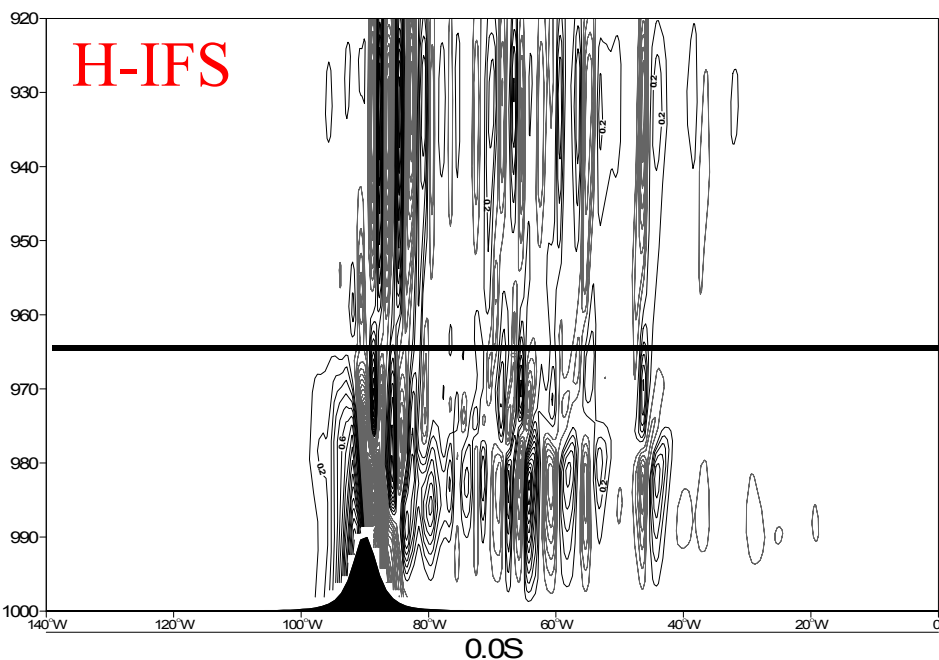
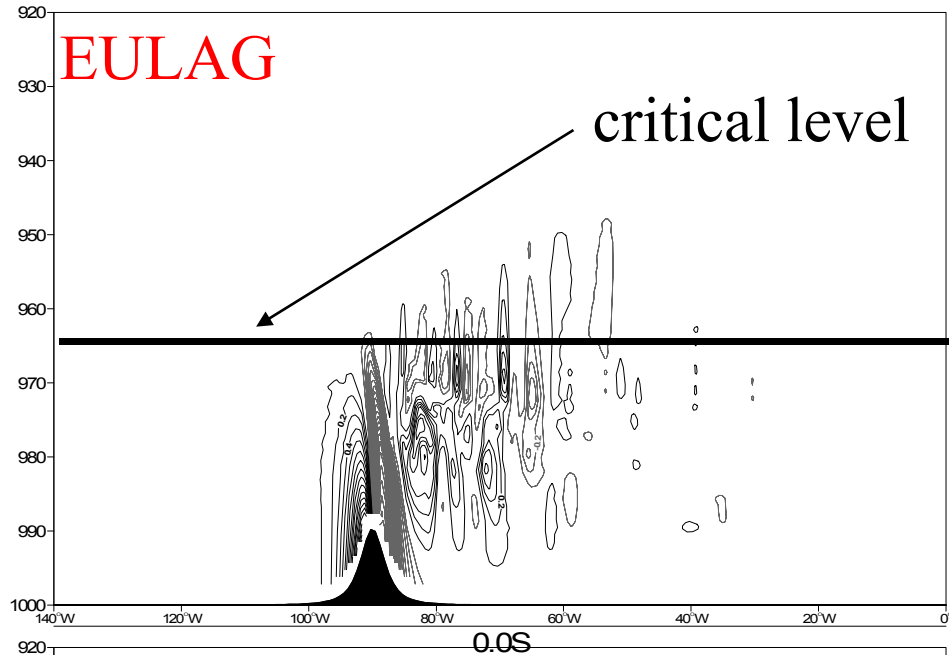


The figures illustrate the correct horizontal (NH) and the (incorrect) vertical (H) propagation of gravity waves in this case (Keller, 1994). Shown is vertical velocity.

(Wedi and Smolarkiewicz, 2009)

The critical level effect on linear and non-linear flow past a three-dimensional hill

LS5
$$\frac{U_0}{NL_\lambda} = 1$$



Skewness and (excess) Kurtosis (250hPa vorticity)

Variance:

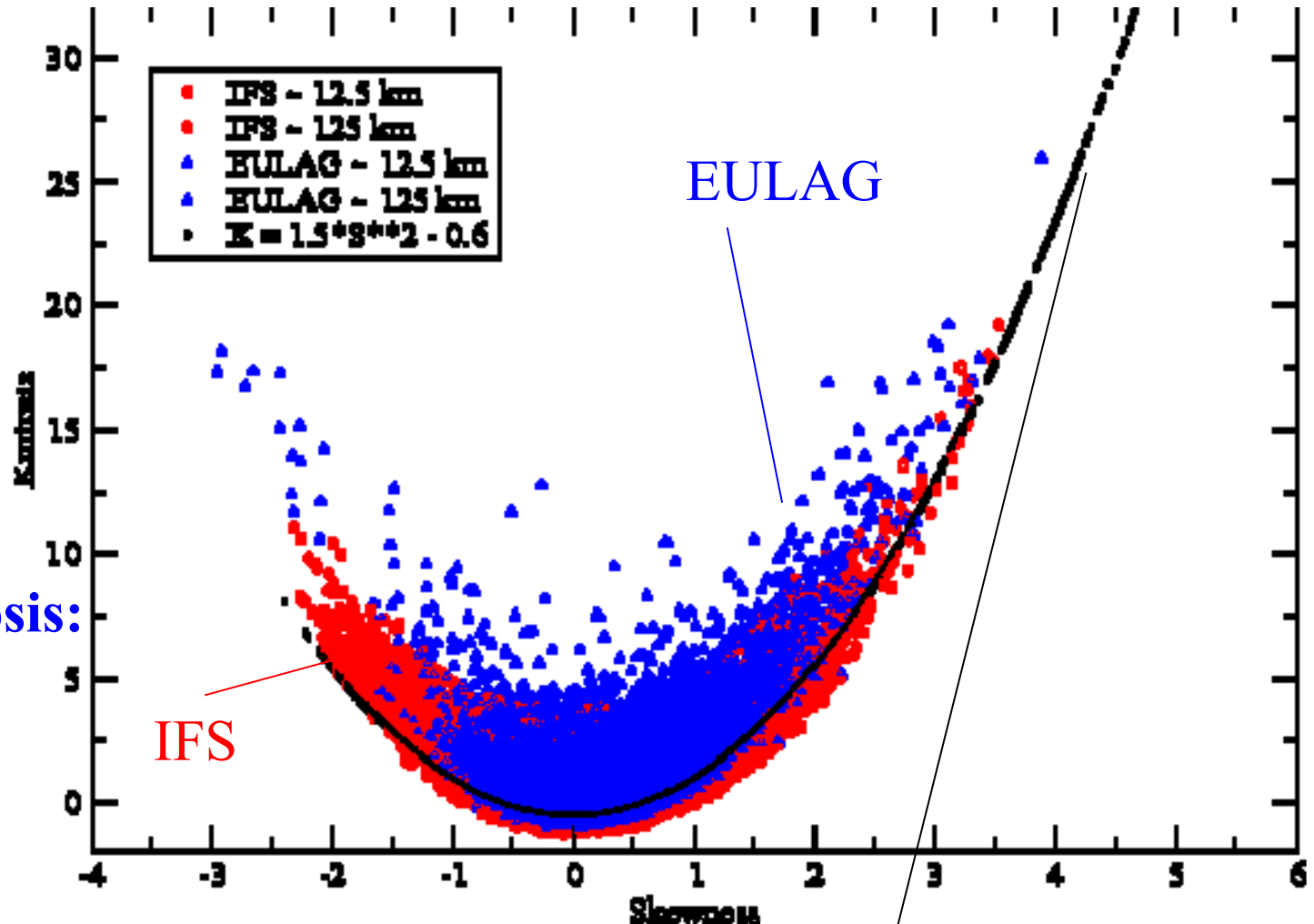
$$\sigma = \overline{(x - \bar{x})^2}$$

Skewness:

$$s = \frac{\overline{(x - \bar{x})^3}}{\sigma^{3/2}}$$

(excess) Kurtosis:

$$k = \frac{\overline{(x - \bar{x})^4}}{\sigma^2} - 3$$



Predicted from linear stochastic models

forced with non-Gaussian noise (Sardeshmukh and Surda, 2009)

Higher resolution influence (250hPa vorticity)

Variance:

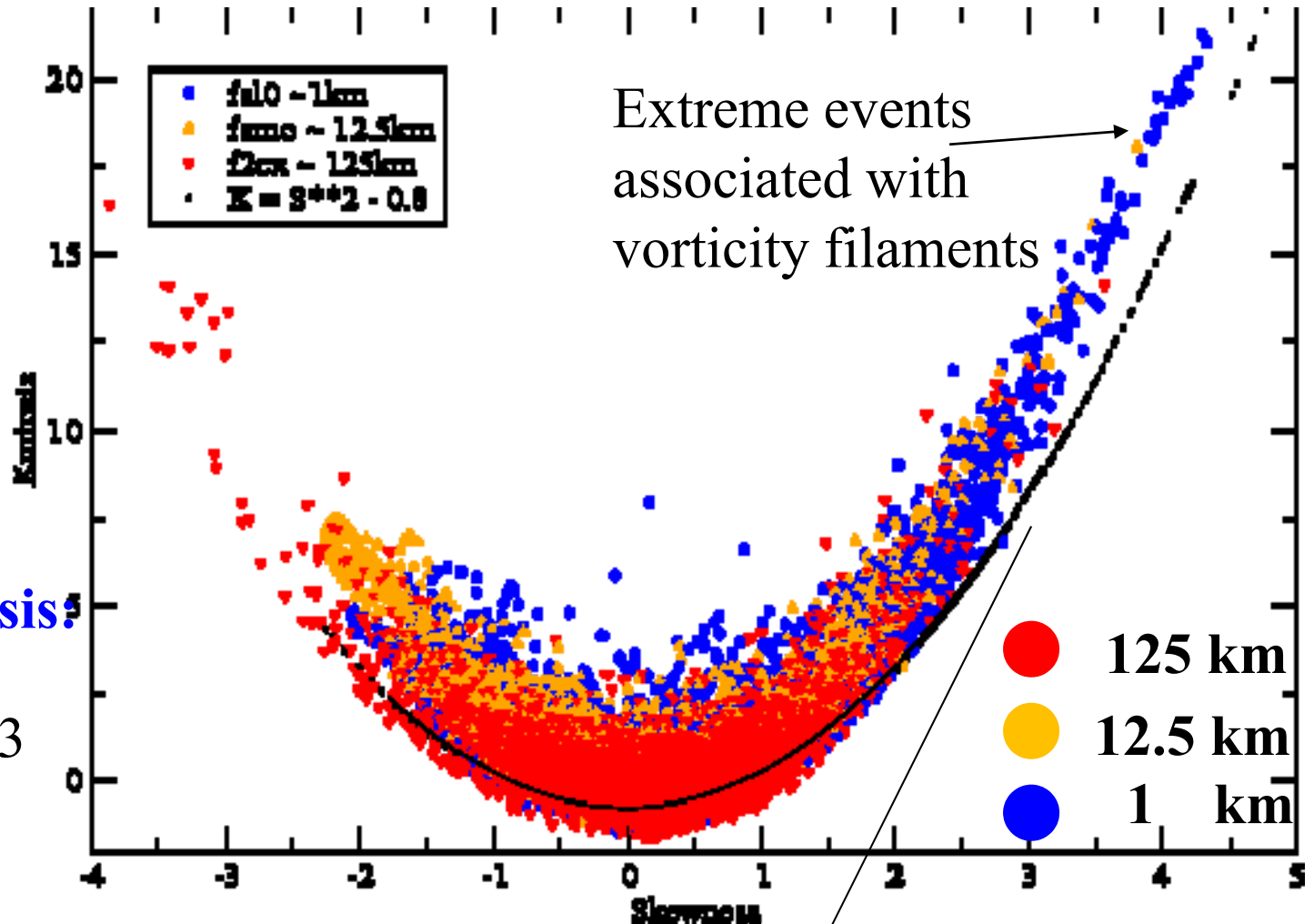
$$\sigma = \overline{(x - \bar{x})^2}$$

Skewness:

$$s = \frac{\overline{(x - \bar{x})^3}}{\sigma^{3/2}}$$

(excess) Kurtosis:

$$k = \frac{\overline{(x - \bar{x})^4}}{\sigma^2} - 3$$



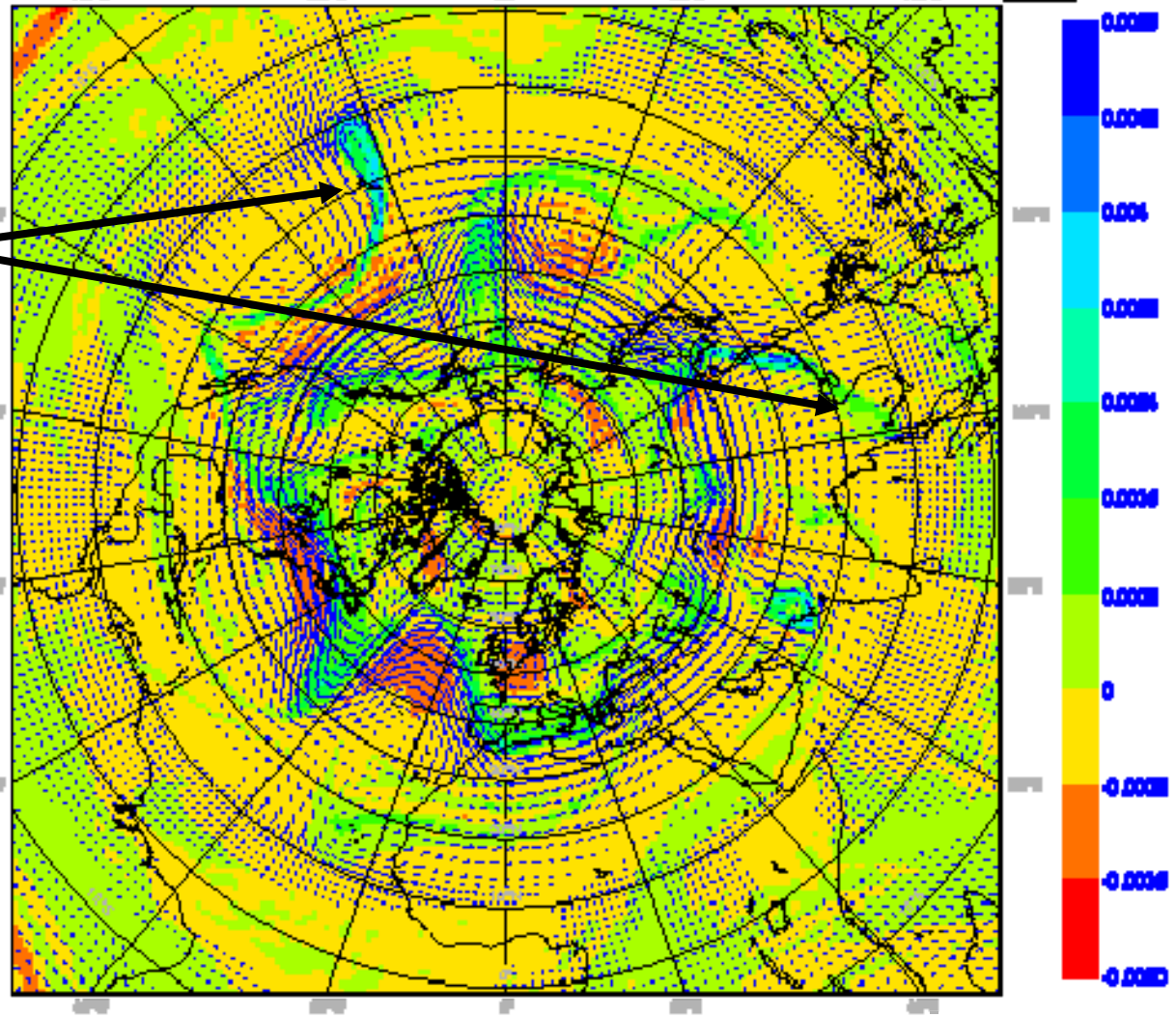
Predicted from linear stochastic models

forced with non-Gaussian noise (Sardeshmukh and Surda, 2009)

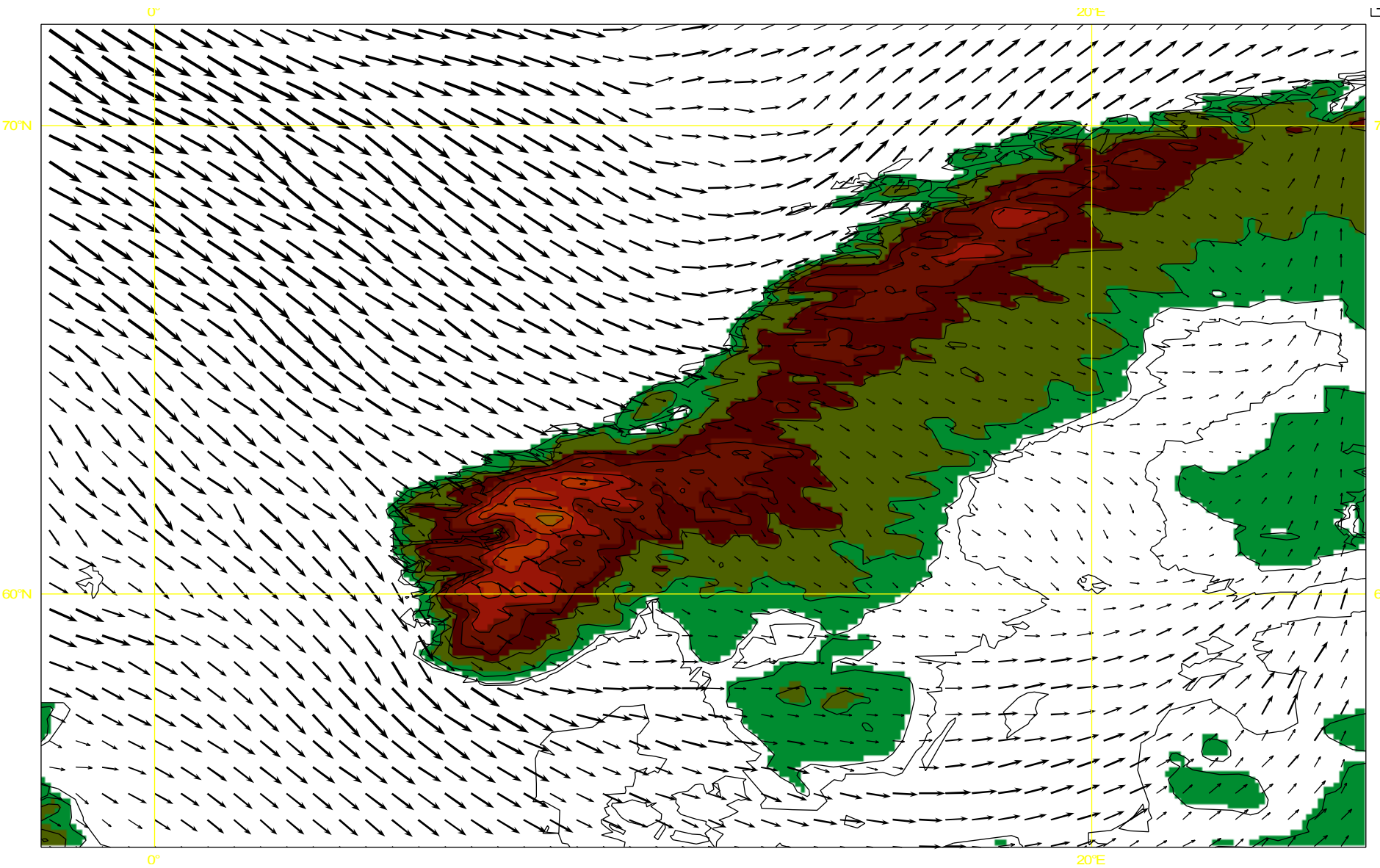
Cyclonic vorticity (extreme events)

ECMWF | PROGRAMS AND SERVICES | METEOROLOGICAL PRODUCTS | DATA SERVICES | RESEARCH AND DEVELOPMENT | TRAINING | ABOUT | CONTACT | LEGAL | TERMS AND CONDITIONS | PRIVACY POLICY | WEBSITE | HELP | SEARCH | HOME

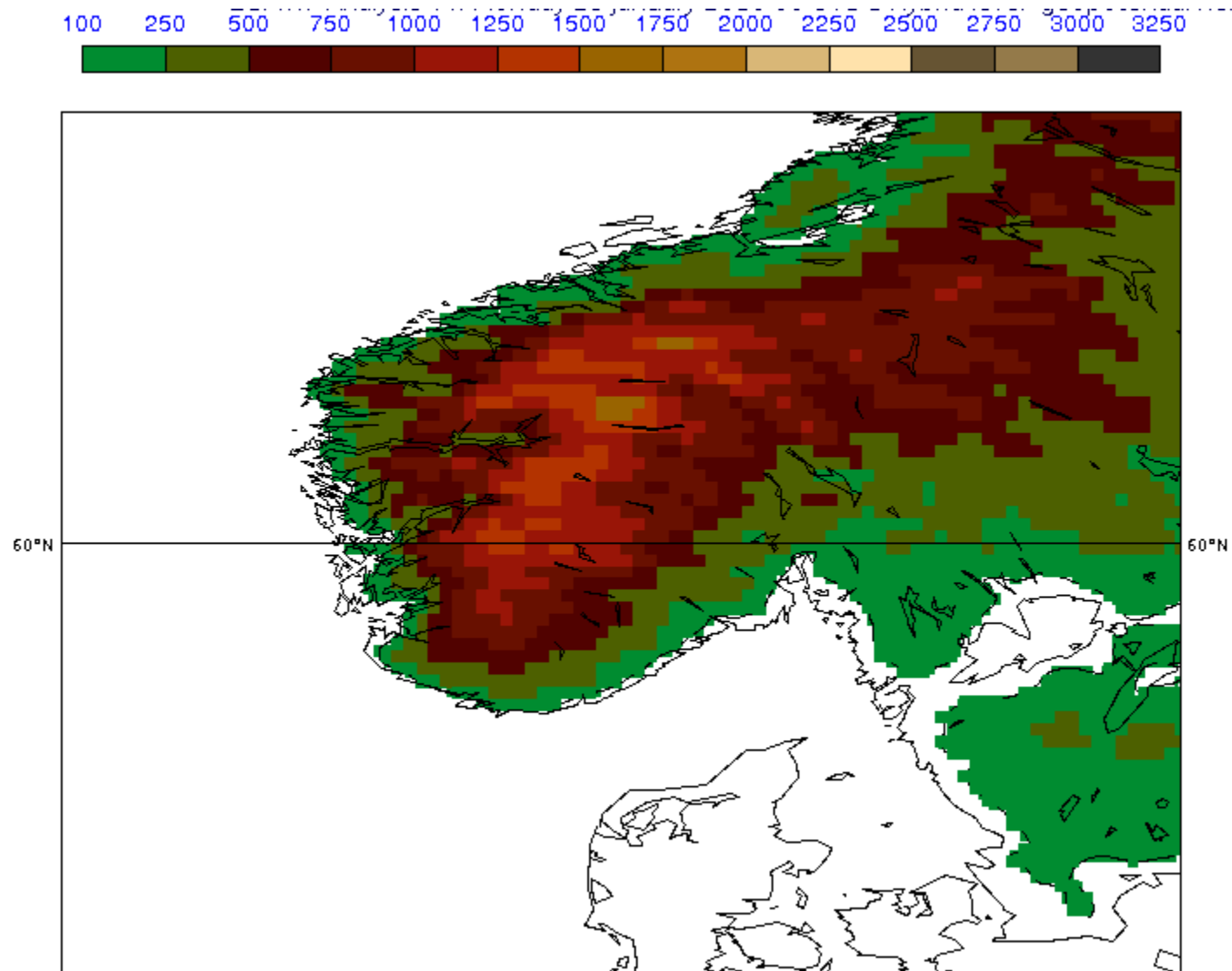
Tuesday 1 August 2023 12:17:03 BST/04:00 UTC Forecast by 144 VTI Monday 7 August 2023 12:17:03 BST/04:00 UTC (UTC+0)



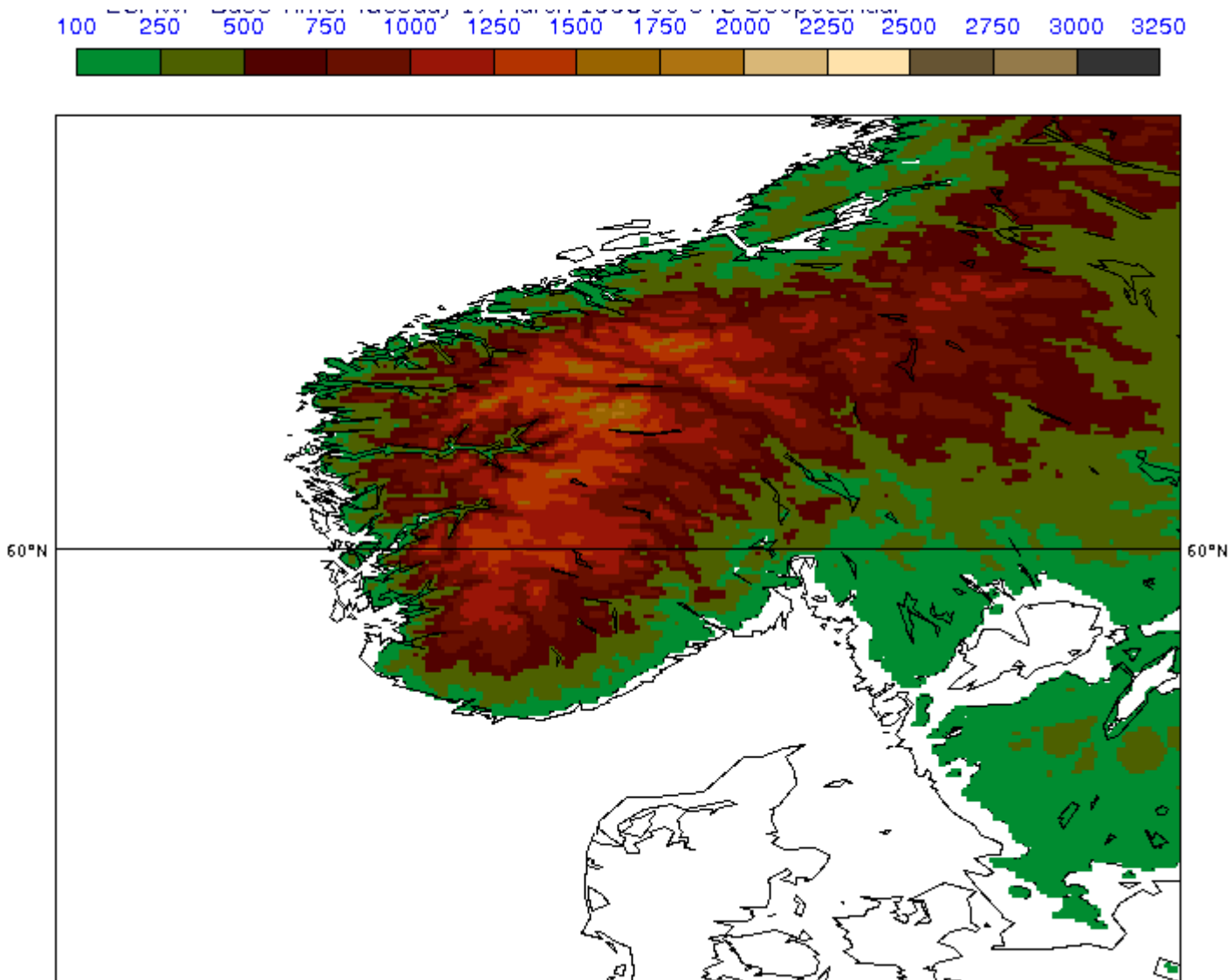
For example *vorticity filaments* are associated with high skewness and high (excess) kurtosis !



Orography – T1279

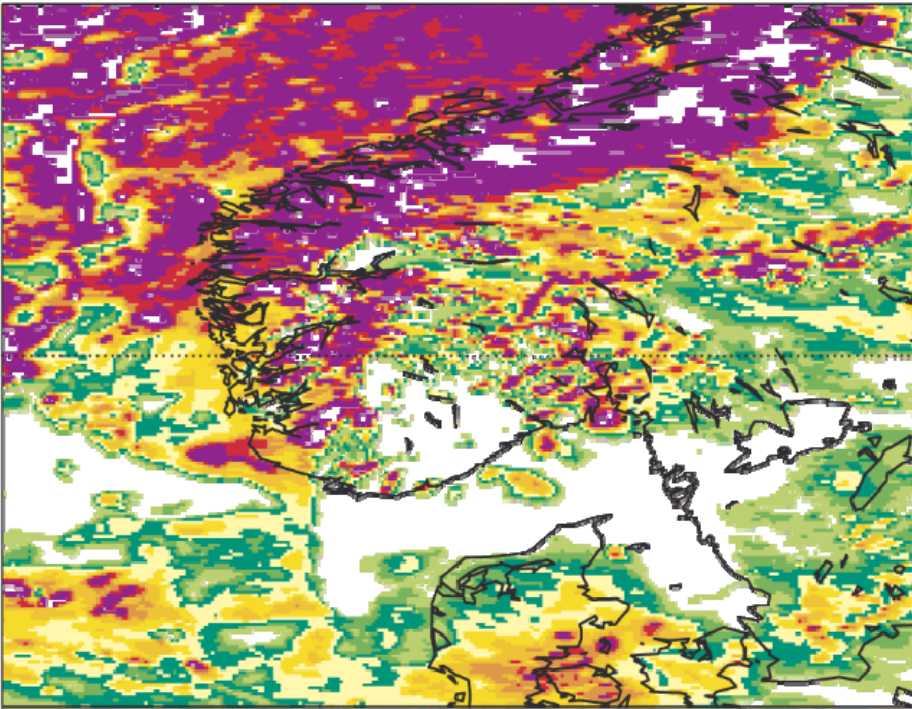


Orography T3999

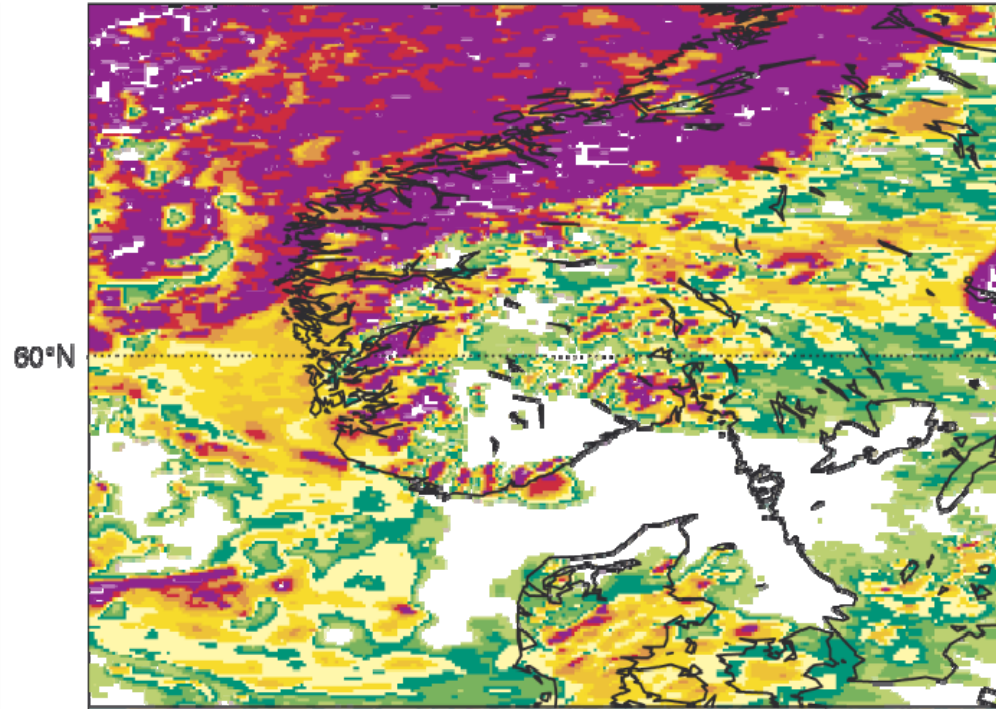


Cloud cover 24h forecast T3999 (~5km)

a Non-hydrostatic simulation

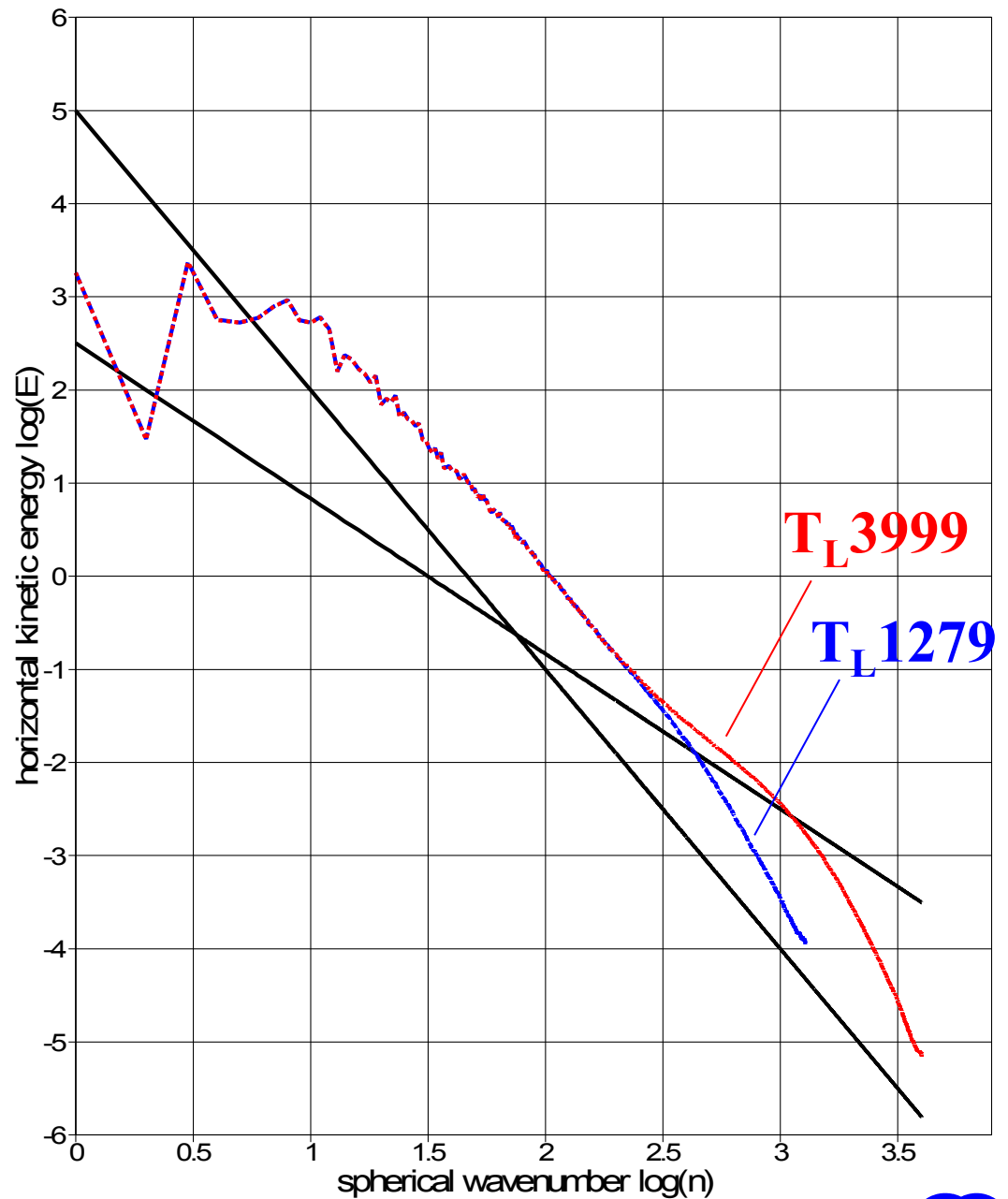


b Hydrostatic simulation



Era-Interim shows a wind shear with height in the troposphere over the region!

Kinetic Energy Spectra (500hPa) T3999 – T1279



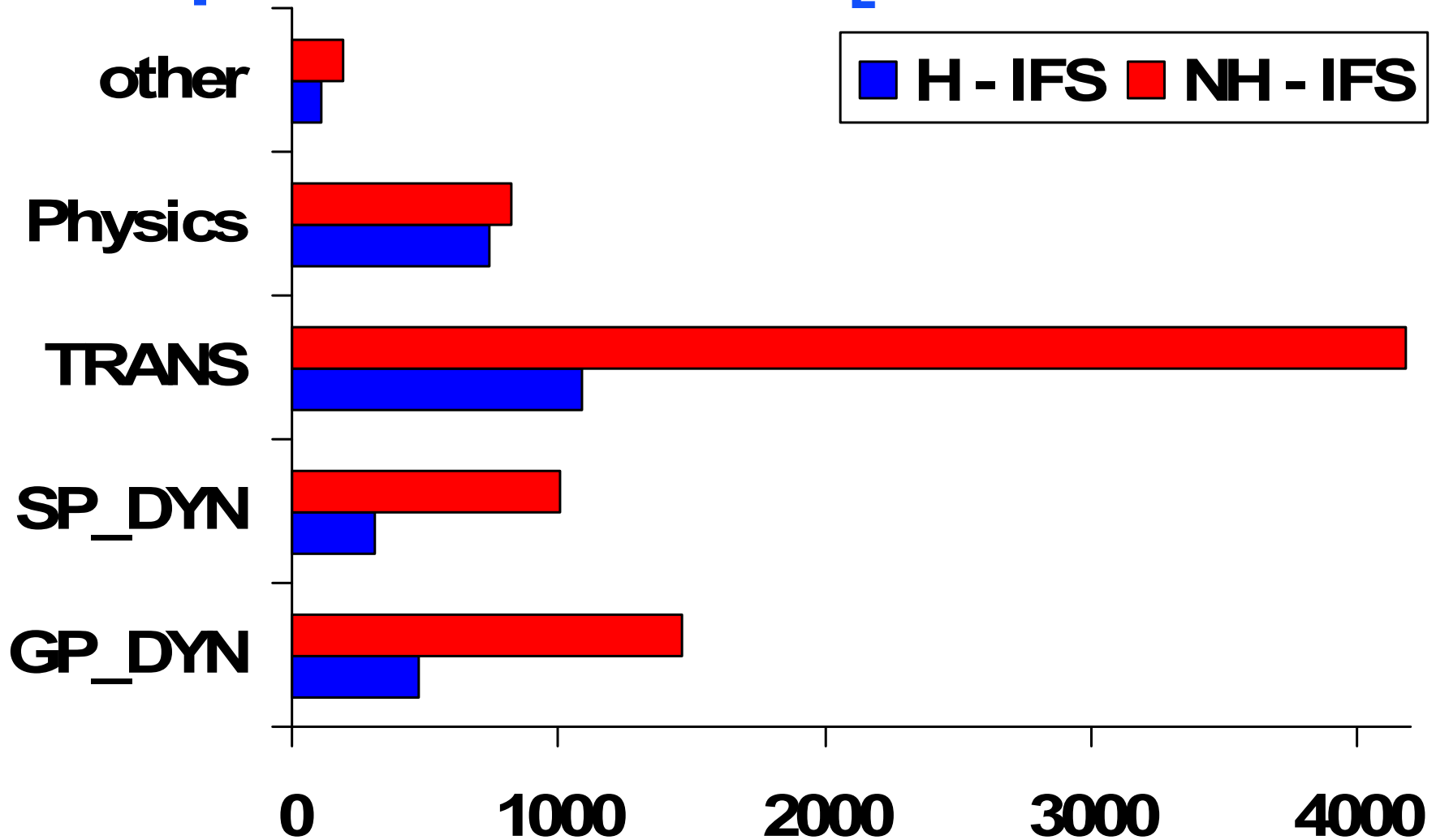
Kinetic Energy Spectra (10hPa)

T3999 – T1279

H IFS

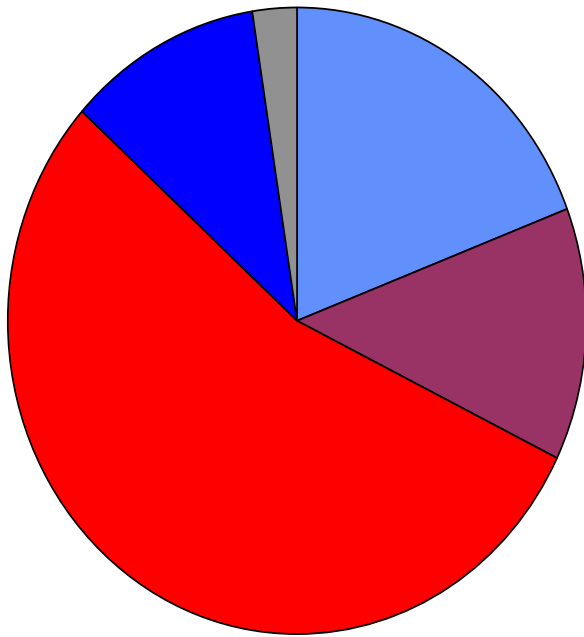


Computational Cost at T_L3999

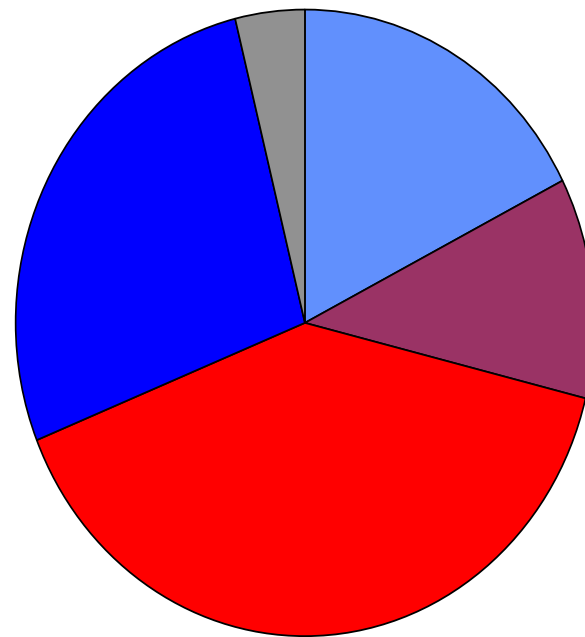


Total cost increase for 24h forecast: H 50min vs. NH 150min

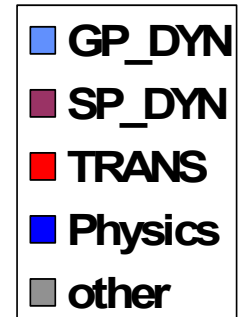
Computational Cost at T_L3999 hydrostatic vs. non-hydrostatic IFS



NH T_L3999

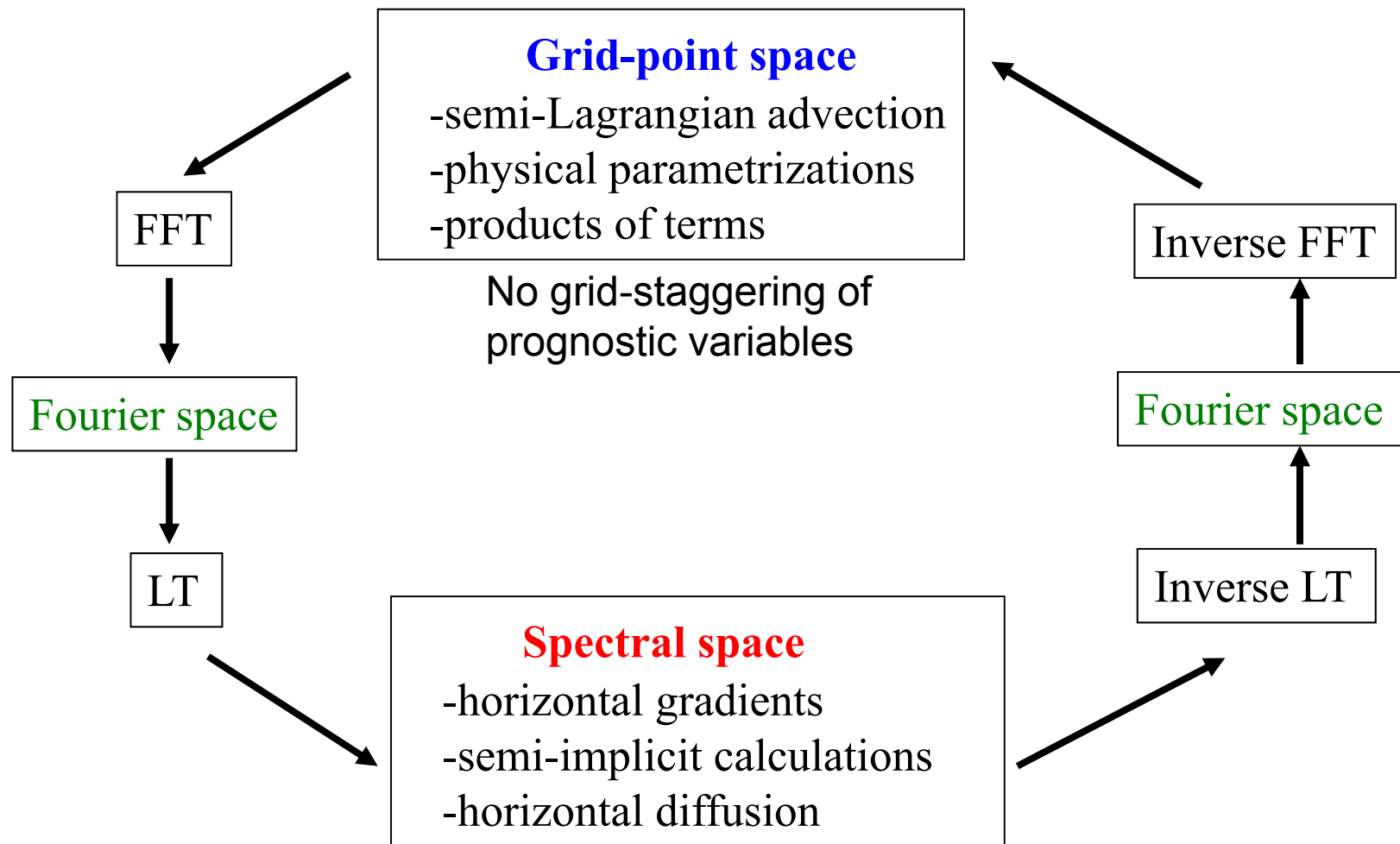


H T_L3999



The spectral transform method

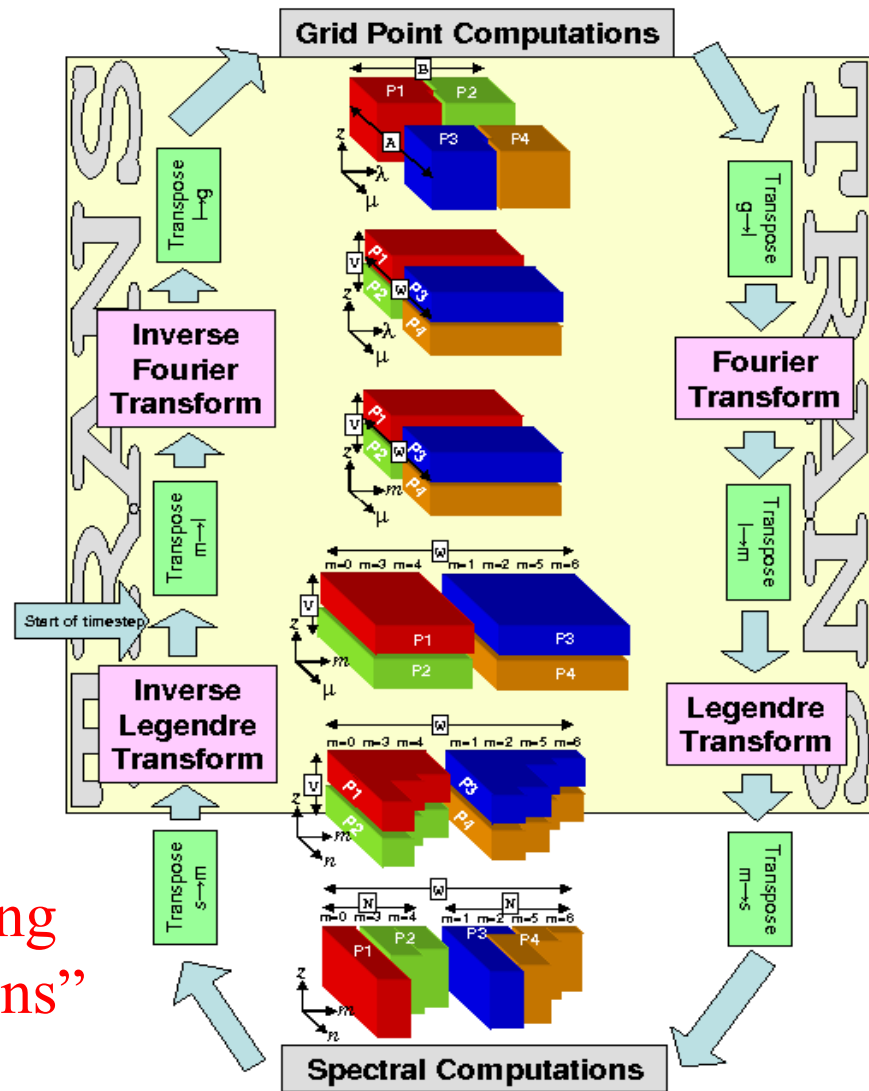
Schematic description of the **spectral transform method** in the **ECMWF IFS model**



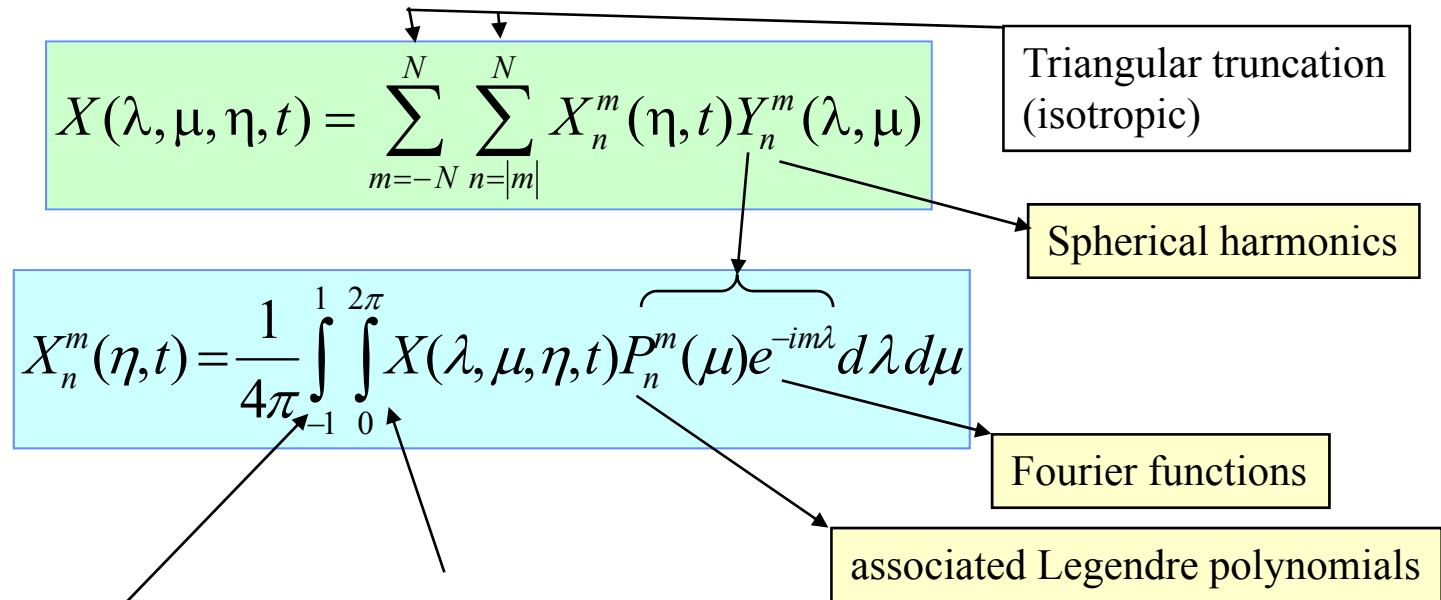
FFT: Fast Fourier Transform, LT: Legendre Transform

Transpositions within the spectral transforms

The time spent in message passing associated with the “transpositions” at T1279 is roughly equal to the computational time.



Horizontal discretisation of variable X (e.g. temperature)



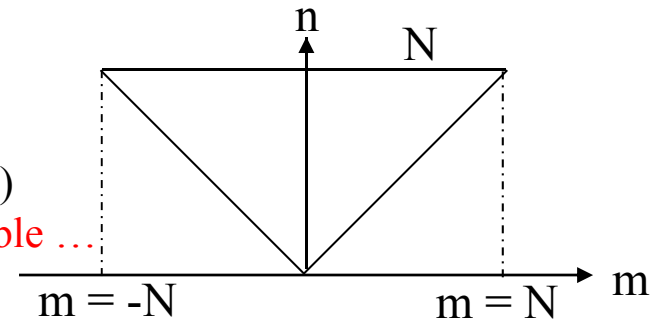
Legendre transform

by Gaussian quadrature
 using $N_L \geq (2N+1)/2$
 “Gaussian” latitudes (linear grid)
 $((3N+1)/2$ if quadratic grid)
 “fast” algorithm desirable ...

FFT (fast Fourier transform)

using
 $N_F \geq 2N+1$
 points (linear grid)
 $(3N+1$ if quadratic grid)
 “fast” algorithm available ...

Triangular truncation:



Computation of the associated Legendre polynomials

- ◆ Increase of error due to recurrence formulae (Belousov, 1962)
- ◆ Recent changes to transform package went into cycle 35r3 that allow the computation of Legendre functions and Gaussian latitudes in double precision following ([Schwarztrauber, 2002](#)) and increased accuracy 10^{-13} instead of 10^{-12} .
- ◆ **Note:** the increased accuracy leads in the “*Courtier and Naughton* (1994) procedure for the reduced Gaussian grid” to slightly more points near the poles for all resolutions.
- ◆ **Note:** At resolutions \geq T3999 the associated Legendre polynomials for large m get very small ...

Cost of the spectral transform method

- ◆ FFT can be computed as $C*N*\log(N)$ where C is a small positive number and N is the cut-off wave number in the triangular truncation.
- ◆ Ordinary Legendre transform is $O(N^2)$ but can be combined with the fields/levels such that the arising matrix-matrix multiplies make use of the highly optimized BLAS routine DGEMM.
- ◆ But overall cost is $O(N^3)$ for both memory and CPU time requirements.

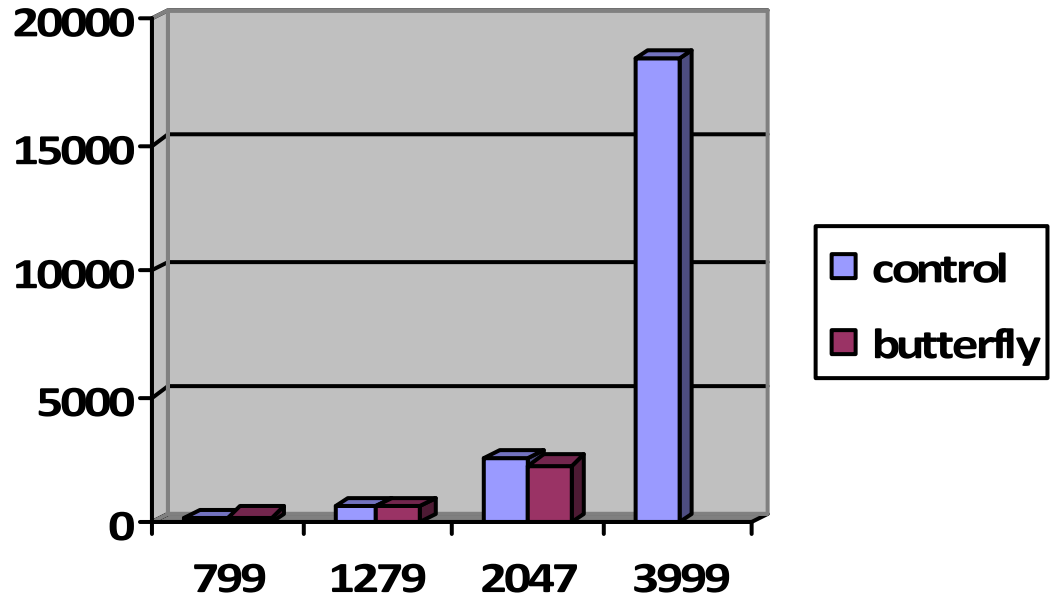
➔ Desire to use a fast Legendre transform where the cost is proportional to $C*N*\log(N)$ with $C \ll N$

and thus overall cost $N^2*\log(N)$

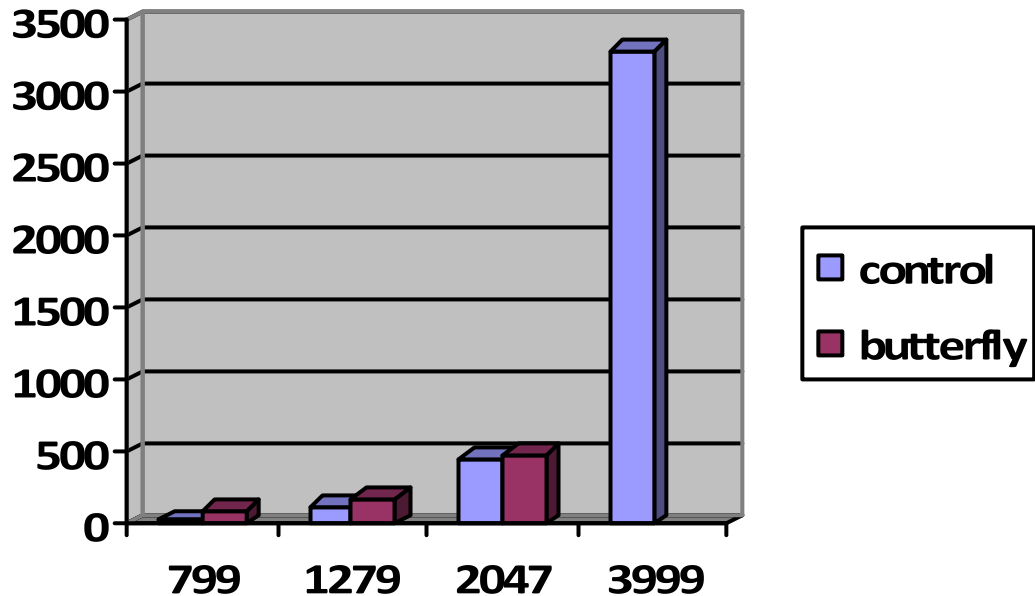
Fast Legendre transform

- ◆ The algorithm proposed in (*Tygert, 2008*) suitably fits into the IFS transform library by simply replacing the single DGEMM call with 2 new steps plus more expensive pre-computations.
- ◆ (1) Instead of the recursive *Cuppen divide-and-conquer algorithm* (*Tygert, 2008*) we use the so called *butterfly algorithm* (*Tygert, 2010*) based on a matrix compression technique via rank reduction with a specified accuracy to accelerate the arising *matrix-vector multiplies (sub-problems still use dgemm)*.
- ◆ (2) The arising interpolation from one set of roots of the associated Legendre polynomials to another can be accelerated by using a *FMM (fast multipole method)*.

Floating point operations per time-step in Gflop



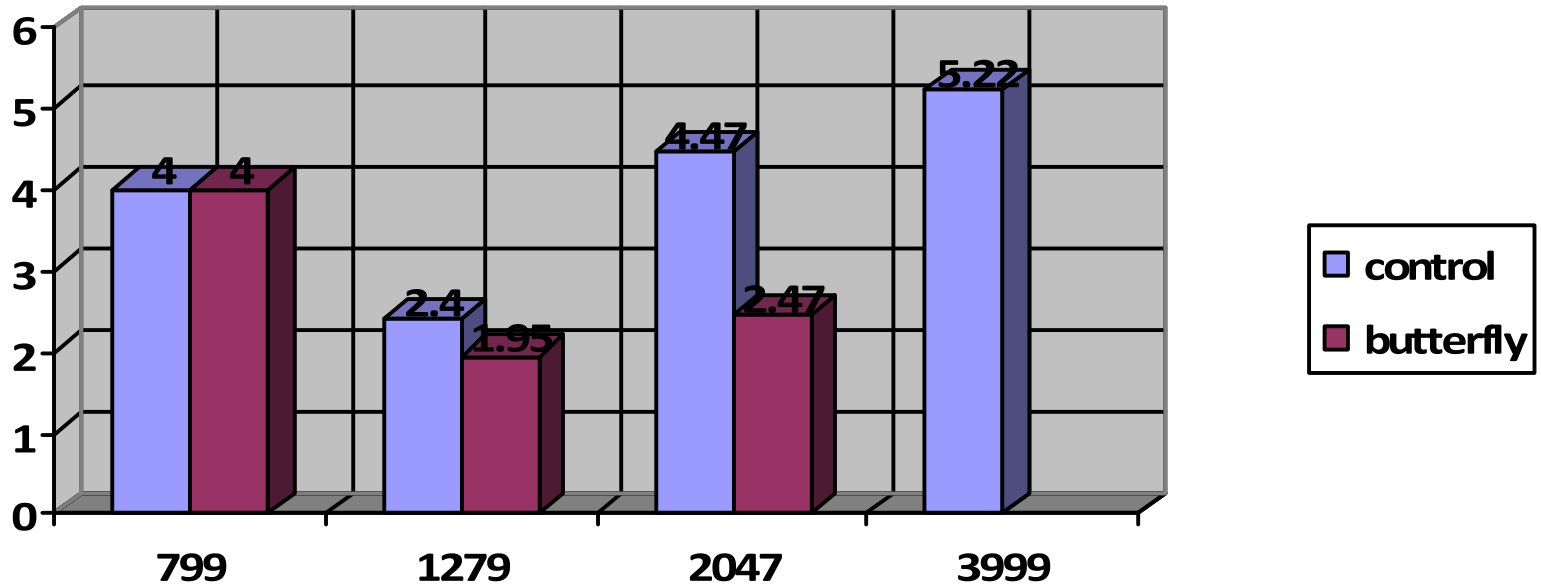
Computational cost per time-step in seconds



Inverse transform only

Average elapsed time

for a single ordinary model time-step with typical configurations on the IBM power6



799	1279	2047	3999
288	1536	4096/8192	8448
48x6	192x8	512x8/16	528x16
$\Delta t = 720s$	$\Delta t = 600s$	$\Delta t = 450s$	$\Delta t = 240s$

Towards a unified hydrostatic-anelastic IFS system

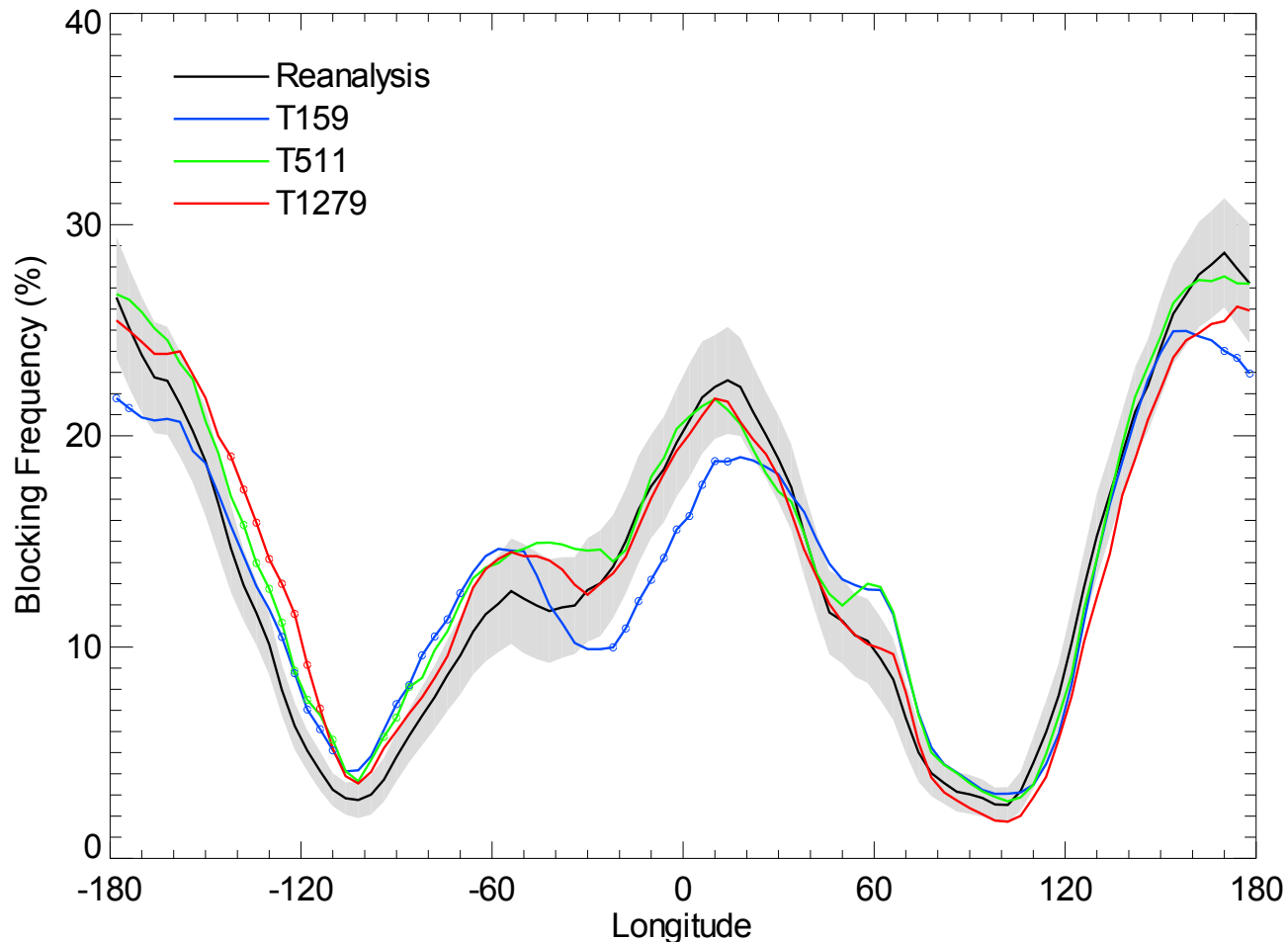
- ◆ Scientifically, the benefit of having a prognostic equation for non-hydrostatic pressure departure is unclear.
- ◆ The coupling to the physics is ambiguous.
- ◆ For stability reasons, the NH system requires at least one iteration, which essentially doubles the number of spectral transforms.
- ◆ Given the cost of the spectral transforms, any reduction in the number of prognostic variables will save costs.

Summary and outlook

- ◆ “Pushing the boundaries” with first T_L3999 simulations.
- ◆ The non-hydrostatic IFS works robust at hydrostatic scales with equivalently large time-steps compared to the hydrostatic IFS.
- ◆ However, computational cost (almost 3 x at T_L3999) is a serious issue ! Even with the hydrostatic IFS at T_L3999 the conventional spectral computations are about 50% of the total computing time.
- ◆ Fast Legendre Transform (*Tygert, 2008,2010*) shows some promise but to be evaluated further.
- ◆ The unified IFS hydrostatic-anelastic equations (*Arakawa and Konor, 2009*) may be a way forward towards highly efficient and stable integrations for the hydrostatic and the non-hydrostatic regime (see also the next talk by Pierre).

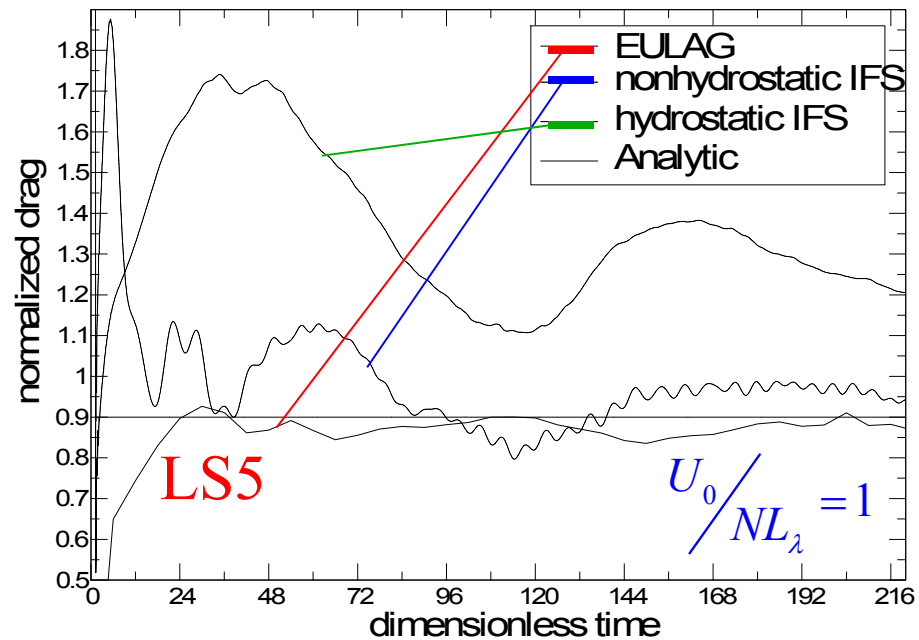
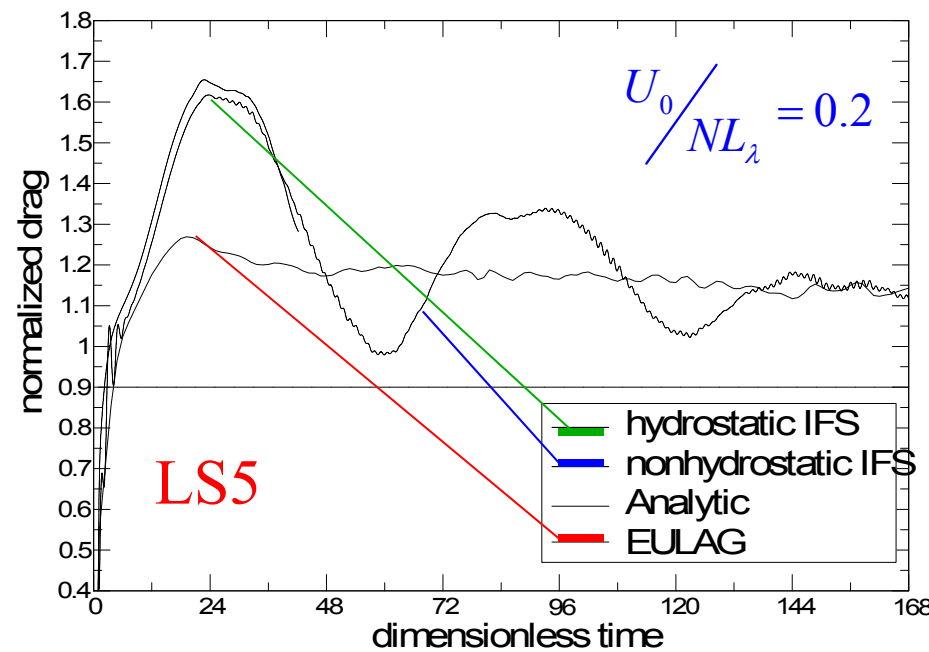
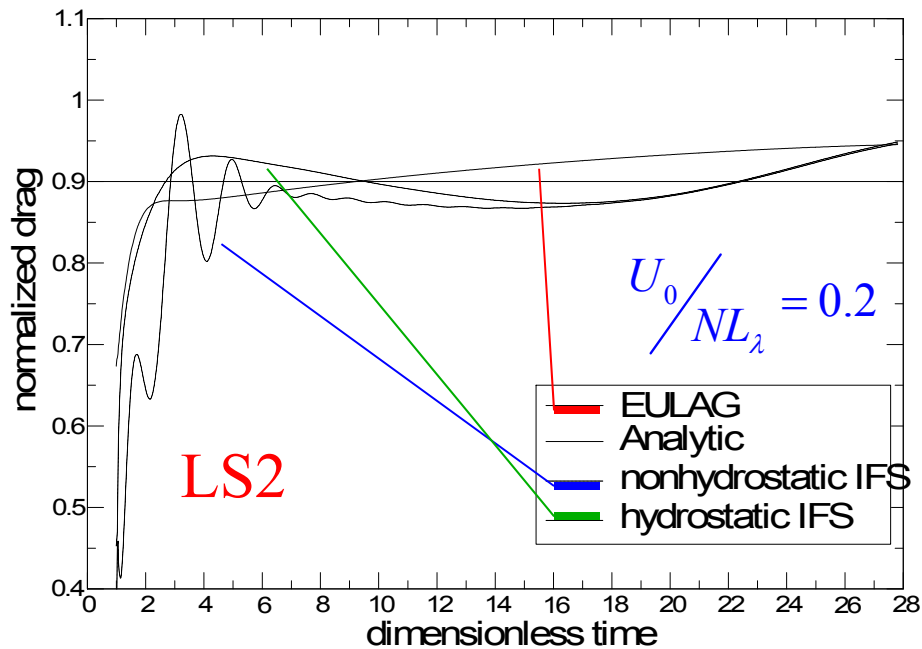
Additional slides

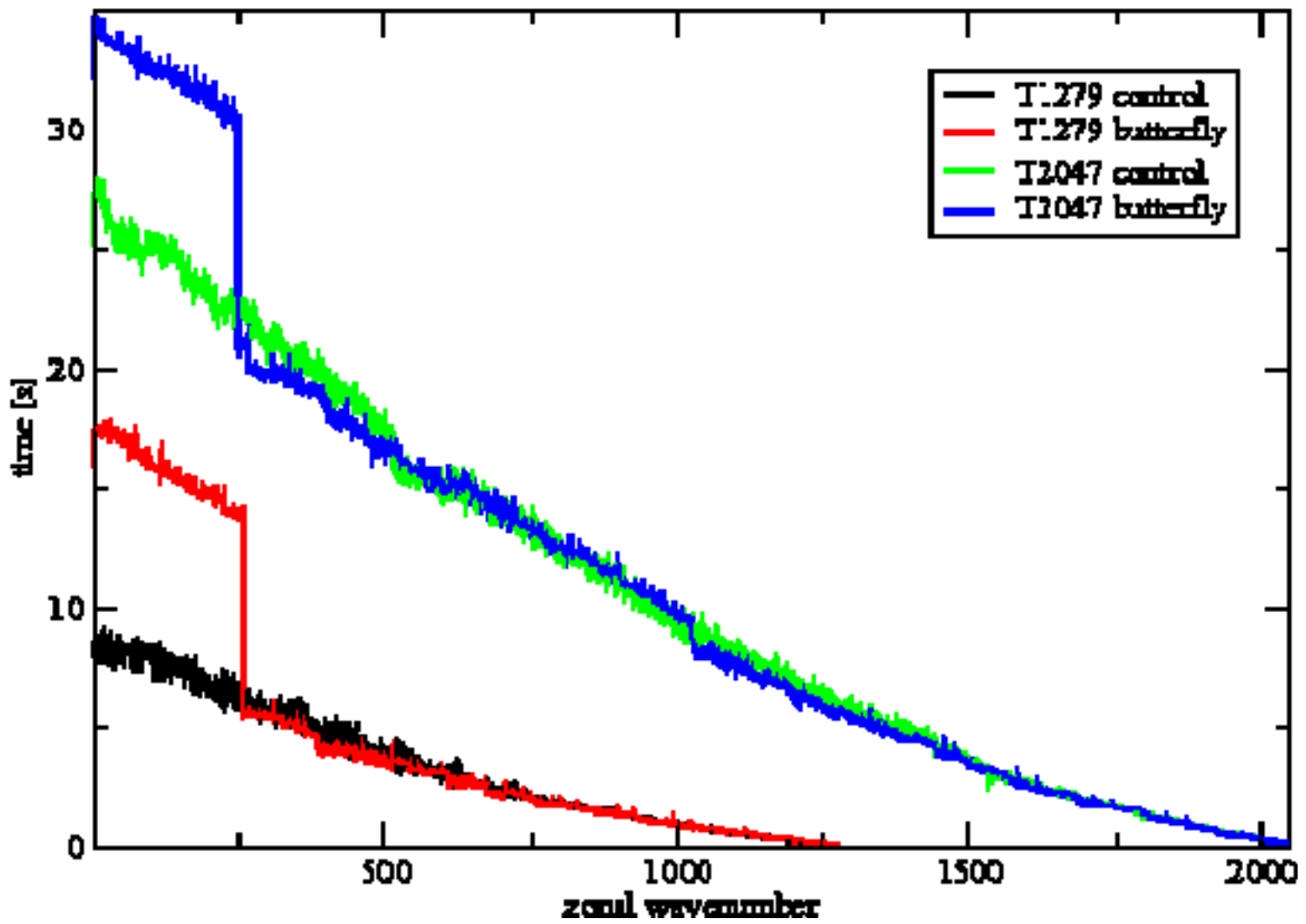
The Athena project



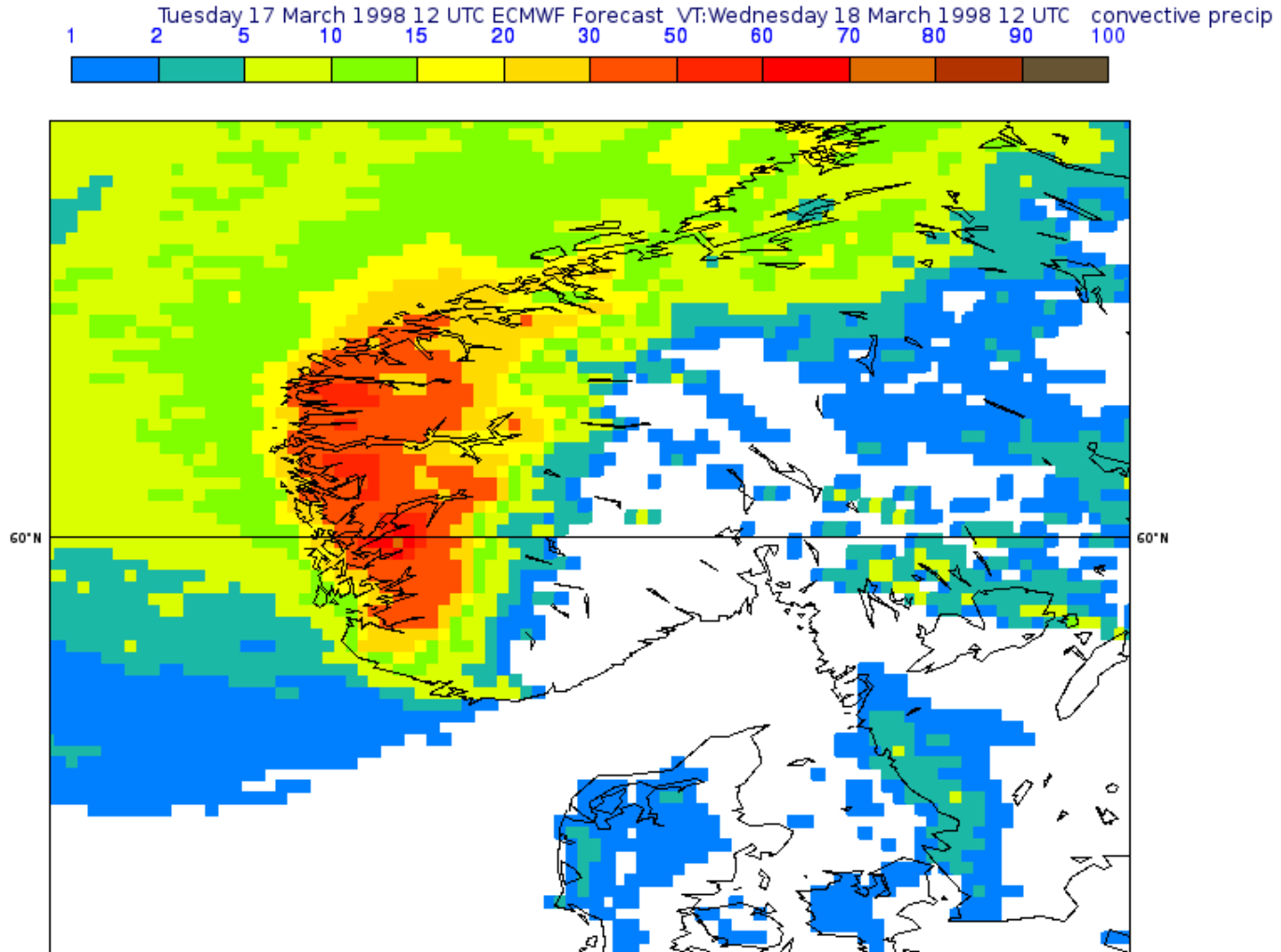
Atmospheric blocking (DJFM 1960-2007)

Mountain drag

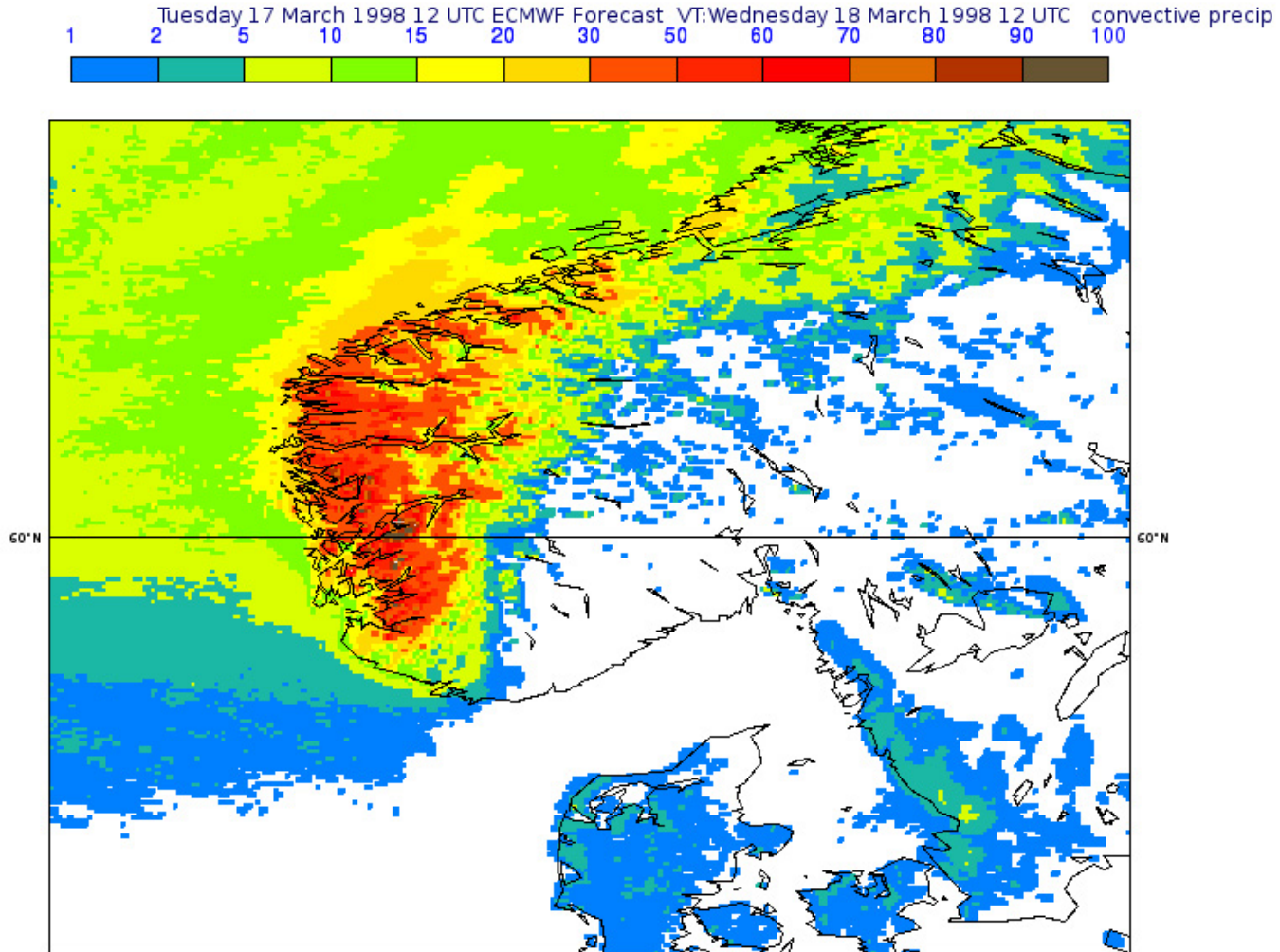




T1279 Precipitation

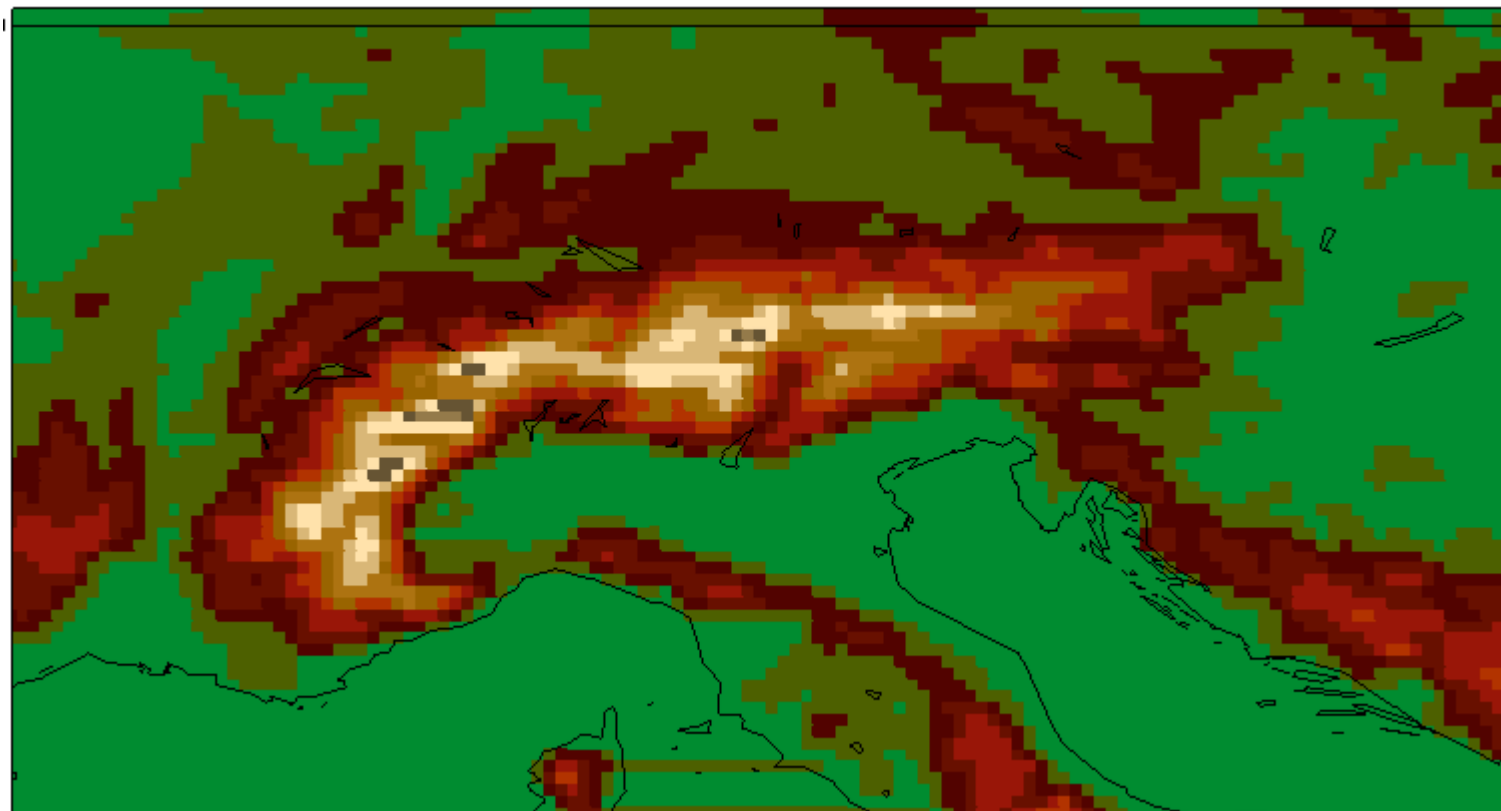


T3999 precipitation



Max global altitude = 6503m

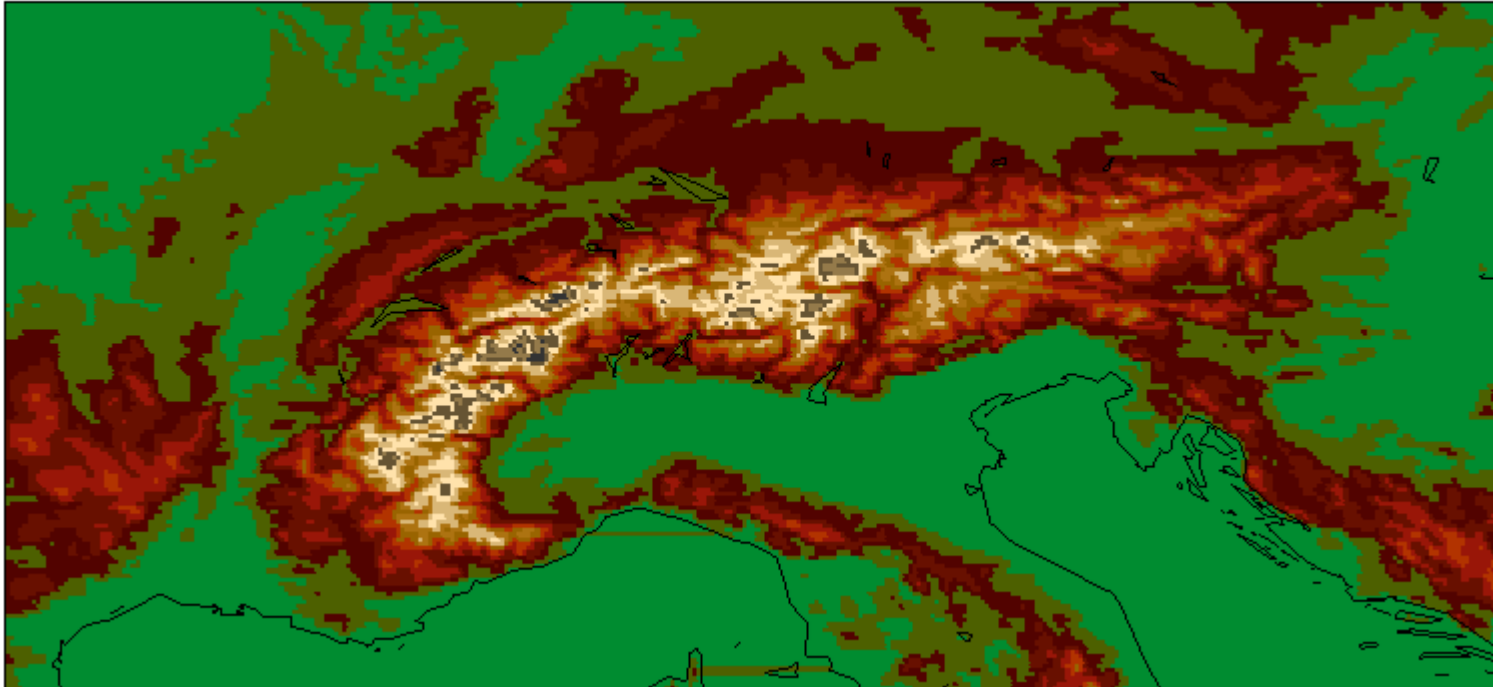
Orography – T1279



Alps

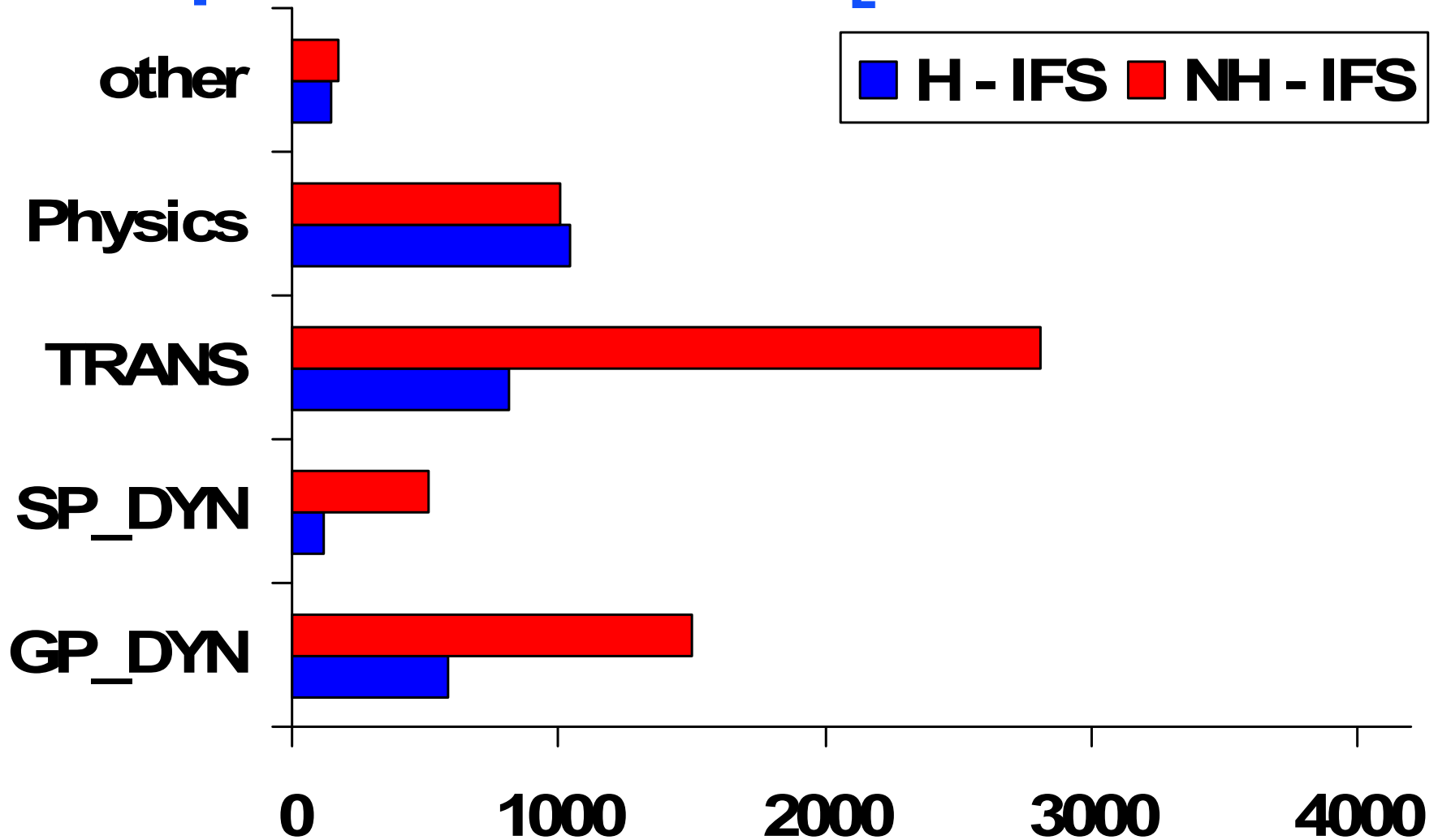
Max global altitude = 7185m

Orography - T3999



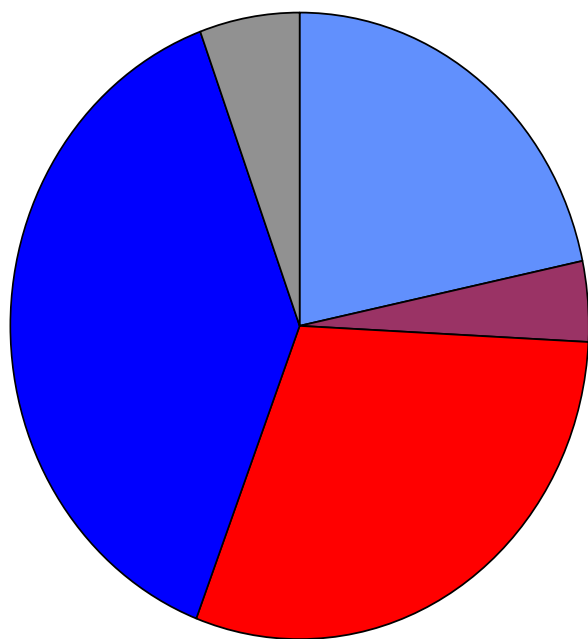
Alps

Computational Cost at T_L2047

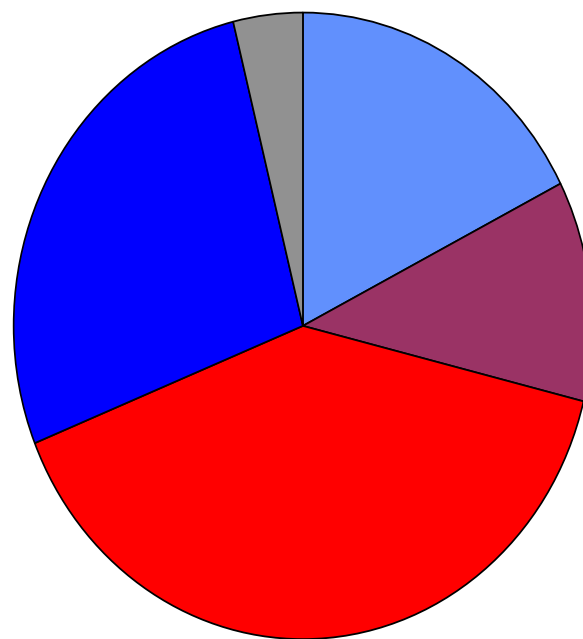


Total cost increase NH – H 106 %

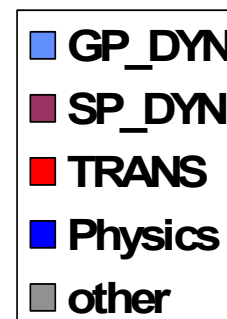
Computational Cost at T_L2047 and T_L3999 (with the hydrostatic IFS)



H T_L2047



H T_L3999



Numerical solution

- ◆ Advection via a two-time-level semi-Lagrangian numerical technique as in the hydrostatic system.
- ◆ Semi-implicit procedure with two reference states with respect to gravity and acoustic waves, respectively.
- ◆ The resulting Helmholtz equation is more complicated than in the hydrostatic case but can still be solved (subject to some constraints on the vertical discretization) with a direct solver as before.

(Benard et al 2004,2005,2010)

Vertical coordinate

$$\pi = A(\eta) + B(\eta)\pi_s(\lambda, \phi, t)$$

hybrid vertical coordinate

Simmons and Burridge (1981)

Denotes hydrostatic pressure in the context of a shallow, vertically unbounded planetary atmosphere.

Prognostic surface pressure tendency:

$$\frac{\partial \pi_s}{\partial t} = - \int_0^1 \nabla_{\eta} \cdot (m \mathbf{v}_h) d\eta,$$

with $m \equiv \partial \pi / \partial \eta$

coordinate transformation coefficient

Diagnostic relations

$$\frac{dd}{dt} = d(\nabla_{\eta} \cdot \mathbf{v}_h - D_3) - \frac{gp}{mRT} \left(\frac{\partial(dw/dt)}{\partial\eta} - \nabla_{\eta} w \cdot \frac{\partial\mathbf{v}_h}{\partial\eta} \right)$$

With

$$dw/dt = g\partial(p - \pi)/\partial\pi + P_w$$